infection,[39] thus suggesting that the 158V genotype may possess an immunologically recessive nature in immunocompromised patients similar to transplant recipients. However, precisely how the recipient FCGR3A polymorphism influences the pathophysiology of GVHD is still unknown. The first assumption is that in the light of the pathogenesis of GVHD,[40,41] differential binding of IgG to FCGR3A on recipient DCs might alter downstream events, such as the release of cytokines or chemokines, which consecutively could influence pathway essential for the development of GVHD. The second assumption is that the expression of FCGR3A on keratinocytes[42] may have a role in neutralizing the autoantibodies contributing to GVHD.

An alternative explanation is that the association between the recipient FCGR3A polymorphism and the transplant outcomes could develop from polymorphisms in other genes in linkage disequilibrium with the FCGR3A gene. One possible candidate is the Fcγ receptor IIA (FCGR2A) H131R polymorphism shown to be in linkage disequilibrium with the FCGR3A polymorphism in the Caucasian populations.[31,43] However, the absence of a linkage disequilibrium between FCGR3A and FCGR2A genes in Japanese population[31] suggests that the FCGR3A polymorphism is more likely responsible for the transplant outcomes.

The current data are not consistent with a previous French study[44] that found no significant association between the FCGR3A-V158F SNP polymorphism and transplant outcomes. One of the reasons for this discrepancy may be that the population in the initial study included only HLA-identical sibling BMT recipients and was not stratified into myeloid and lymphoid malignancies to examine the effect of gene polymorphism on transplant outcomes. There is a possibility that the influence of the FCGR3A polymorphism is restricted exclusively to unrelated BMT and myeloid malignancies. Alternatively, these conflicting findings may result from ethnic differences in the study population. Verification of the present data in other cohorts has still to be made so that the implications of the findings can be fully accepted.

This study suggests that the genotyping of FCGR3A in transplant recipients before transplantation may provide a recipient bearing the 158F/F genotype an opportunity to avoid the risk of GVHD by favoring a BM or cord blood, and an HLA-matched graft, and planning more immunosuppressive regimens. Further studies are required to ascertain whether the findings of this study can be extended to other disease groups or other stem sources or HLA-mismatched transplantation.

Conflict of interest

The authors declare no conflict of interest.

Acknowledgements

We are indebted to Drs Hiroko Oshima, Masanobu Oshima and Atsushi Hirao, Ms Kayoko Yamada, Mayu Yamada and Yuki Motohashi at Kanazawa University, and Dr Keitaro Matsuo at Aichi Cancer Center Research Institute for their technical assistance. We thank all the Japan Marrow Donor Program (JMDP) transplant teams who have contributed patients and donors to this study. This study was supported by grants from the Ministry of Health, Labor and Welfare, and the Ministry of Education, Culture, Sports and Technology, and Funds from the Mitani Research and Development Assistance Organization (Kanazawa, Japan) and by the Japan Leukemia Research Fund (Tokyo, Japan).

References

1 Gratwohl A, Brand R, Frassoni F, Rocha V, Niederwieser D, Reusser P *et al.* Cause of death after allogeneic haematopoietic stem cell transplantation (HSCT) in early leukaemias: an EBMT analysis of lethal infectious complications and changes over calendar time. *Bone Marrow Transplant* 2005; **36**: 757–769.
2 Dickinson AM, Middleton PG, Rocha V, Gluckman E, Holler E. Genetic polymorphisms predicting the outcome of bone marrow transplants. *Br J Haematol* 2004; **127**: 479–490.
3 Elmaagacli AH, Koldehoff M, Landt O, Beelen DW. Relation of an interleukin-23 receptor gene polymorphism to graft-versus-host disease after hematopoietic-cell transplantation. *Bone Marrow Transplant* 2008; **41**: 821–826.
4 Gerbitz A, Hillemanns P, Schmid C, Wilke A, Jayaraman R, Kolb HJ *et al.* Influence of polymorphism within the heme oxygenase-I promoter on overall survival and transplantation-related mortality after allogeneic stem cell transplantation. *Biol Blood Marrow Transplant* 2008; **14**: 1180–1189.
5 Kim DH, Jung HD, Lee NY, Sohn SK. Single nucleotide polymorphism of CC chemokine ligand 5 promoter gene in recipients may predict the risk of chronic graft-versus-host disease and its severity after allogeneic transplantation. *Transplantation* 2007; **84**: 917–925.
6 Noori-Daloii MR, Rashidi-Nezhad A, Izadi P, Hossein-Nezhad A, Sobhani M, Derakhshandeh-Peykar P *et al.* Transforming growth factor-beta1 codon 10 polymorphism is associated with acute GVHD after allogenic BMT in Iranian population. *Ann Transplant* 2007; **12**: 5–10.
7 Viel DO, Tsuneto LT, Sossai CR, Lieber SR, Marques SB, Vigorito AC *et al.* IL2 and TNFA gene polymorphisms and the risk of graft-versus-host disease after allogeneic haematopoietic stem cell transplantation. *Scand J Immunol* 2007; **66**: 703–710.
8 Sugimoto K, Murata M, Onizuka M, Inamoto Y, Terakura S, Kuwatsuka Y *et al.* Decreased risk of acute graft-versus-host disease following allogeneic hematopoietic stem cell transplantation in patients with the 5,10-methylenetetrahydrofolate reductase 677TT genotype. *Int J Hematol* 2008; **87**: 451–458.
9 Espinoza JL, Takami A, Onizuka M, Sao H, Akiyama H, Miyamura K *et al.* NKG2D gene polymorphism has a significant impact on transplant outcomes after HLA-fully-matched unrelated bone marrow transplantation for standard risk hematologic malignancies. *Haematologica* 2009; **94**: 1427–1434.
10 Nimmerjahn F, Ravetch JV. Fcgamma receptors: old friends and new family members. *Immunity* 2006; **24**: 19–28.
11 Nimmerjahn F, Ravetch JV. Fcgamma receptors as regulators of immune responses. *Nat Rev Immunol* 2008; **8**: 34–47.
12 Shimabukuro-Vornhagen A, Hallek MJ, Storb RF, von Bergwelt-Baildon MS. The role of B cells in the pathogenesis of graft-versus-host disease. *Blood* 2009; **114**: 4919–4927: blood-2008-10-161638.
13 Cauza K, Grassauer A, Hinterhuber G, Horvat R, Rappersberger K, Wolff K *et al.* FcgammaRIII expression on cultured

human keratinocytes and upregulation by interferon-gamma. *J Invest Dermatol* 2002; **119**: 1074–1079.

14 Leppers-van de Straat FG, van der Pol WL, Jansen MD, Sugita N, Yoshie H, Kobayashi T *et al.* A novel PCR-based method for direct Fc gamma receptor IIIa (CD16) allotyping. *J Immunol Methods* 2000; **242**: 127–132.

15 Koene HR, Kleijer M, Algra J, Roos D, von dem Borne AE, de Haas M. Fc gammaRIIIa-158V/F polymorphism influences the binding of IgG by natural killer cell Fc gammaRIIIa, independently of the Fc gammaRIIIa-48 L/R/H phenotype. *Blood* 1997; **90**: 1109–1114.

16 Wu J, Edberg JC, Redecha PB, Bansal V, Guyre PM, Coleman K *et al.* A novel polymorphism of FcgammaRIIIa (CD16) alters receptor function and predisposes to autoimmune disease. *J Clin Invest* 1997; **100**: 1059–1070.

17 Tutuncu Z, Kavanaugh A, Zvaifler N, Corr M, Deutsch R, Boyle D. Fcgamma receptor type IIIA polymorphisms influence treatment outcomes in patients with inflammatory arthritis treated with tumor necrosis factor alpha-blocking agents. *Arthritis Rheum* 2005; **52**: 2693–2696.

18 Foster CB, Zhu S, Erichsen HC, Lehrnbecher T, Hart ES, Choi E *et al.* Polymorphisms in inflammatory cytokines and Fcgamma receptors in childhood chronic immune thrombocytopenic purpura: a pilot study. *Br J Haematol* 2001; **113**: 596–599.

19 Cartron G, Dacheux L, Salles G, Solal-Celigny P, Bardos P, Colombat P *et al.* Therapeutic activity of humanized anti-CD20 monoclonal antibody and polymorphism in IgG Fc receptor FcgammaRIIIa gene. *Blood* 2002; **99**: 754–758.

20 Weng WK, Levy R. Two immunoglobulin G fragment C receptor polymorphisms independently predict response to rituximab in patients with follicular lymphoma. *J Clin Oncol* 2003; **21**: 3940–3947.

21 Sugita N, Yamamoto K, Kobayashi T, Van Der Pol W, Horigome T, Yoshie H *et al.* Relevance of Fc gamma RIIIa-158V-F polymorphism to recurrence of adult periodontitis in Japanese patients. *Clin Exp Immunol* 1999; **117**: 350–354.

22 Dijstelbloem HM, Bijl M, Fijnheer R, Scheepers RH, Oost WW, Jansen MD *et al.* Fcgamma receptor polymorphisms in systemic lupus erythematosus: association with disease and *in vivo* clearance of immune complexes. *Arthritis Rheum* 2000; **43**: 2793–2800.

23 Zhang W, Gordon M, Schultheis AM, Yang DY, Nagashima F, Azuma M *et al.* FCGR2A and FCGR3A polymorphisms associated with clinical outcome of epidermal growth factor receptor expressing metastatic colorectal cancer patients treated with single-agent cetuximab. *J Clin Oncol* 2007; **25**: 3712–3718.

24 Kawase T, Morishima Y, Matsuo K, Kashiwase K, Inoko H, Saji H *et al.* High-risk HLA allele mismatch combinations responsible for severe acute graft-versus-host disease and implication for its molecular mechanism. *Blood* 2007; **110**: 2235–2241.

25 Sasazuki T, Juji T, Morishima Y, Kinukawa N, Kashiwabara H, Inoko H *et al.* Effect of matching of class I HLA alleles on clinical outcome after transplantation of hematopoietic stem cells from an unrelated donor. Japan Marrow Donor Program. *N Engl J Med* 1998; **339**: 1177–1185.

26 Livak KJ. Allelic discrimination using fluorogenic probes and the 5′ nuclease assay. *Genet Anal* 1999; **14**: 143–149.

27 Przepiorka D, Weisdorf D, Martin P, Klingemann HG, Beatty P, Hows J *et al.* 1994 Consensus conference on acute GVHD grading. *Bone Marrow Transplant* 1995; **15**: 825–828.

28 Shulman HM, Sullivan KM, Weiden PL, McDonald GB, Striker GE, Sale GE *et al.* Chronic graft-versus-host syndrome in man. A long-term clinicopathologic study of 20 Seattle patients. *Am J Med* 1980; **69**: 204–217.

29 Scrucca L, Santucci A, Aversa F. Competing risk analysis using R: an easy guide for clinicians. *Bone Marrow Transplant* 2007; **40**: 381–387.

30 Gooley TA, Leisenring W, Crowley J, Storer BE. Estimation of failure probabilities in the presence of competing risks: new representations of old estimators. *Stat Med* 1999; **18**: 695–706.

31 van der Pol WL, Jansen MD, Sluiter WJ, van de Sluis B, Leppers-van de Straat FG, Kobayashi T *et al.* Evidence for non-random distribution of Fcgamma receptor genotype combinations. *Immunogenetics* 2003; **55**: 240–246.

32 Schultz KR, Paquet J, Bader S, HayGlass KT. Requirement for B cells in T cell priming to minor histocompatibility antigens and development of graft-versus-host disease. *Bone Marrow Transplant* 1995; **16**: 289–295.

33 Kamble R, Oholendt M, Carrum G. Rituximab responsive refractory acute graft-versus-host disease. *Biol Blood Marrow Transplant* 2006; **12**: 1201–1202.

34 Zhang C, Todorov I, Zhang Z, Liu Y, Kandeel F, Forman S *et al.* Donor CD4+ T and B cells in transplants induce chronic graft-versus-host disease with autoimmune manifestations. *Blood* 2006; **107**: 2993–3001.

35 Cutler C, Miklos D, Kim HT, Treister N, Woo SB, Bienfang D *et al.* Rituximab for steroid-refractory chronic graft-versus-host disease. *Blood* 2006; **108**: 756–762.

36 Rowe V, Banovic T, MacDonald KP, Kuns R, Don AL, Morris ES *et al.* Host B cells produce IL-10 following TBI and attenuate acute GVHD after allogeneic bone marrow transplantation. *Blood* 2006; **108**: 2485–2492.

37 Storek J, Wells D, Dawson MA, Storer B, Maloney DG. Factors influencing B lymphopoiesis after allogeneic hematopoietic cell transplantation. *Blood* 2001; **98**: 489–491.

38 Michonneau D, Peffault de Latour R, Porcher R, Robin M, Benbunan M, Rocha V *et al.* Influence of bone marrow graft B lymphocyte subsets on outcome after HLA-identical sibling transplants. *Br J Haematol* 2009; **145**: 107–114.

39 Lehrnbecher TL, Foster CB, Zhu S, Venzon D, Steinberg SM, Wyvill K *et al.* Variant genotypes of Fcgamma RIIIA influence the development of Kaposi's sarcoma in HIV-infected men. *Blood* 2000; **95**: 2386–2390.

40 Ferrara JL, Cooke KR, Teshima T. The pathophysiology of acute graft-versus-host disease. *Int J Hematol* 2003; **78**: 181–187.

41 Teshima T, Ordemann R, Reddy P, Gagin S, Liu C, Cooke KR *et al.* Acute graft-versus-host disease does not require alloantigen expression on host epithelium. *Nat Med* 2002; **8**: 575–581.

42 Cauza K, Grassauer A, Hinterhuber G, Horvat R, Rappersberger K, Wolff K *et al.* Fc[gamma]RIII expression on cultured human keratinocytes and upregulation by interferon-[gamma]. *J Invest Dermatol* 2002; **119**: 1074–1079.

43 Lejeune J, Thibault G, Ternant D, Cartron G, Watier H, Ohresser M. Evidence for linkage disequilibrium between Fcgamma RIIIa-V158F and Fcgamma RIIa-H131R polymorphisms in white patients, and for an Fcgamma RIIIa-restricted influence on the response to therapeutic antibodies. *J Clin Oncol* 2008; **26**: 5489–5491.

44 Rocha V, Franco RF, Porcher R, Bittencourt H, Silva Jr WA, Latouche A *et al.* Host defense and inflammatory gene polymorphisms are associated with outcomes after HLA-identical sibling bone marrow transplantation. *Blood* 2002; **100**: 3908–3918.

CARCIN	bgq185	VN
Journal Name	Art. No.	CE Code

Carcinogenesis vol.0 no.0 pp.1–10, 2010
doi:10.1093/carcin/bgq185
Advance Access publication September 7, 2010

The FOXM1 transcriptional factor promotes the proliferation of leukemia cells through modulation of cell cycle progression in acute myeloid leukemia

Satoki Nakamura[1,*,†], Isao Hirano[1,2,†], Keiji Okinaka[1,2], Tomonari Takemura[1,2], Daisuke Yokota[1,2], Takaaki Ono[1,2], Kazuyuki Shigeno[1], Kiyoshi Shibata[3], Shinya Fujisawa[4] and Kazunori Ohnishi[1,2]

[1]Department of Internal Medicine III, [2]Cancer Center and [3]Equipment Center, Hamamatsu University School of Medicine, 1-20-1 Handayama, Higashi-ku, Hamamatsu, Shizuoka 431-3192, Japan and [4]Division of Hematology, Hamamatsu Medical Center, 328 Tomitsuka, Naka-ku, Hamamatsu, Shizuoka 432-8580, Japan

*To whom correspondence should be addressed. Tel: +81 53 435 2267; Fax: +81 53 434 2910;
Email: satonaka@hama-med.ac.jp

FOXM1 is an important cell cycle regulator and regulates cell proliferation. In addition, FOXM1 has been reported to contribute to oncogenesis in various cancers. However, it is not clearly understood how FOXM1 contributes to acute myeloid leukemia (AML) cell proliferation. In this study, we investigated the cellular and molecular function of FOXM1 in AML cells. The *FOXM1* messenger RNA (mRNA) expressed in AML cell lines was predominantly the *FOXM1B* isoform, and its levels were significantly higher than in normal high aldehyde dehydrogenase activity ($ALDH^{hi}$) cells. Reduction of FOXM1 expression in AML cells inhibited cell proliferation compared with control cells, through induction of G_2/M cell cycle arrest, a decrease in the protein expression of Aurora kinase B, Survivin, Cyclin B1, Skp2 and Cdc25B and an increase in the protein expression of $p21^{Cip1}$ and $p27^{Kip1}$. *FOXM1* messenger RNA (mRNA) was overexpressed in all 127 AML clinical specimens tested ($n = 21$, 56, 32 and 18 for M1, M2, M4 and M5 subtypes, respectively). Compared with normal $ALDH^{hi}$ cells, *FOXM1* gene expression was 1.65- to 2.26-fold higher in AML cells. Moreover, the FOXM1 protein was more strongly expressed in AML-derived $ALDH^{hi}$ cells compared with normal $ALDH^{hi}$ cells. In addition, depletion of FOXM1 reduced colony formation of AML-derived $ALDH^{hi}$ cells due to inhibition of *Cdc25B* and *Cyclin B1* expression. In summary, we found that *FOXM1B* mRNA is predominantly expressed in AML cells and that aberrant expression of FOXM1 induces AML cell proliferation through modulation of cell cycle progression. Thus, inhibition of FOXM1 expression represents an attractive target for AML therapy.

Introduction

The forkhead box family of transcription factors consists of >50 mammalian proteins that are characterized by a conserved 100 amino acid winged-helix DNA-binding domain (1–4). Expression of the forkhead box family member FOXM1, which is also known as TRIDENT (5), WIN (6), MPP2 (7) and HFH-11 (8), is induced during the G_1 phase of the cell cycle and its expression continues during S phase and mitosis (9). FOXM1 regulates the transcriptional activity of a number of genes, including the genes encoding cyclin B (10), cyclin A (11,12), Aurora B kinase and Polo-like kinase 1 (13), which are critical for cell cycle progression and mitotic entry. Moreover, FOXM1 regulates the genes encoding CENPA, CENPF, NEK2 and KIF20A, which are essential for mitotic spindle checkpoint integrity (14,15). FOXM1 activity induces $p27^{Kip1}$ and $p21^{Cip1}$ degradation through upregulation of SKP2 and CKS1 (15–17), whereas depletion of FOXM1 expression results in cell cycle arrest, mitotic spindle defects, chromosome misaggregation and mitotic catastrophe (14,15,18). Regarding cell proliferation, it has been reported that FOXM1 promotes tumor progression in malignancies, such as gliomas, breast and colorectal cancers, hepatocellular and prostate carcinomas and lung adenocarcinomas (11,12,14,15,19–21). These results suggest that FOXM1 plays important roles in the oncogenesis of malignancies.

FOXM1 was reported to contribute to cellular transformation through interaction with the human papillomavirus-16 E7 protein, which binds to the cell cycle inhibitory protein pRb (7). Interestingly, the *FOXM1* gene is located on the chromosomal band 12p13 (5), and this band is commonly amplified in advanced-stage cervical squamous carcinomas, in which human papillomavirus-16 has been detected in 50% of the cases (22). There are also a few genes linked to cancer development in this chromosomal region, such as the *TEL/ETV6* oncogene, the *cyclin D2* and *$p27^{Kip1}$* genes and the *ING4* tumor suppressor gene. Amplification of the *FOXM1* gene in the presence of human papillomavirus-16 may increase the cell proliferation rate and lead to cancer development (23). Moreover, amplification of the 12p13 locus is frequently found, not only in breast adenocarcinomas (24), nasopharyngeal carcinomas (25) and head and neck squamous cell carcinomas (26) but also in peripheral cytotoxic T cell-lymphomas (27). Also, FOXM1 expression and activity were shown to be significantly elevated by glioma transcription factor-1 (Gli1) through Sonic Hedgehog (Shh) signaling (28) in basal cell carcinoma skin tumors. A recent study of the inactivation of p19ARF, which is a negative regulator of FOXM1, indicated that FOXM1 is required for the proliferative expansion of a variety of tumors. (19). Thus, FOXM1 is inhibited by several tumor suppressor genes, is activated by oncogenes and interference with FOXM1-dependent gene expression is associated with the promotion of tumor development by stimulation of cell cycle progression and cellular proliferation (29). Therefore, the FOXM1 may serve as direct or indirect therapeutic targets. For example, FOXM1 is a target in osteosarcomas and hepatocellular carcinomas (30).

In hematological malignancies, since little is known regarding the function of FOXM1, it is unknown if FOXM1 might be a therapeutic target. It has been reported that *TRIDENT* mRNA is not expressed in peripheral blood lymphocytes but is induced upon stimulation with mitogens *in vitro*, resulting in lymphocyte division (31). Acute myeloid leukemia (AML) is a heterogeneous group of hematologic malignancies that is characterized by a differentiation block in hematopoietic progenitor cells at the early stages of myelopoiesis, which results in the expansion and accumulation of clonal cells that are arrested at various stages of development (32). In particular, aberrant cell cycle controls that normally translate extracellular stimuli into appropriate homeostatic responses can strongly contribute to leukemogenesis by enabling leukemic cells to grow autonomously and escape programmed cell death (33). There is mounting evidence that $p27^{Kip1}$ is very important for control of the proliferation of normal granulocytic cells and macrophages (34). Moreover, the level of $p27^{Kip1}$ is an independent prognostic marker for AML patients, which directly correlates with the survival rate (35). We have reported that KIS induces cell proliferation and cell cycle progression through the phosphorylation of $p27^{Kip1}$ in leukemia cells (36). However, it is unknown if FOXM1 functions as a cell cycle regulator in leukemia cells.

In this study, we investigated the function of FOXM1 in leukemia cell proliferation. We found that aberrant FOXM1 expression promotes the proliferation of both of leukemia cell lines and of leukemic blast cells derived from AML.

Abbreviations: $ALDH^{hi}$, high aldehyde dehydrogenase activity; AML, acute myeloid leukemia; FITC, fluorescein isothiocyanate; MNC, mononuclear cells; mRNA, messenger RNA; PI, propidium iodide; RT-PCR, reverse transcription-polymerase chain reaction.

†These authors contributed equally.

Materials and methods

Cells and cell cultures

The human leukemia cell lines, KG-1, Kasumi-1 and U937, and the human melanoma cell line A375 were purchased from the American Type Culture Collection (Manassas, VA). YRK2 cells were harvested in our laboratory from bone marrow samples of AML (M5a) patients after obtaining informed consent. The KG-1, U937 and YRK2 cells were cultured in RPMI 1640 media containing 10% heat-inactivated fetal bovine serum, 2 mM L-glutamine, 100 μg/ml streptomycin and 200 U/ml penicillin (GIBCO BRL, Gaithersburg, MD). Kasumi-1 cells were grown in RPMI1640 containing 20% fetal bovine serum, 2 mM L-glutamine, 100 μg/ml streptomycin and 200 U/ml penicillin. A375 cells were cultured in Dulbecco's modified Eagle's medium supplemented with 10% fetal bovine serum.

Primary samples

This study analyzed 127 adult patients (age range 34–78 years) with M1 (n = 21), M2 (n = 56), M4 (n = 32) or M5 (n = 18) leukemia (FAB classification). Primary leukemia cell specimens [including bone marrow and peripheral blood mononuclear cells (MNCs)] were obtained from patients before the start of any treatment, and normal hematopoietic cells were extracted from healthy donors after obtaining informed consent. MNCs were purified by Ficoll-Hypaque density gradient centrifugation.

Cell purification based on aldehyde dehydrogenase activity

MNCs were further fractionated according to aldehyde dehydrogenase activity by staining with the Aldefluor reagent (StemCo Biomedical, Durham, NC), according to the manufacturer's specifications. The Aldefluor substrate (0.625 μg/ml) was added to 2 to 7 × 10^6 cells/ml suspended in Aldefluor assay buffer and the cells were then incubated for 20–30 min at 37°C to allow the conversion of the Aldefluor substrate to a fluorescent product that is retained within the cell. The amount of intracellular fluorescence was measured using flow cytometry, and high aldehyde dehydrogenase activity (ALDH^{hi}) cells were selected using a fluorescence-activated cell sorter (Becton Dickinson, San Jose, CA).

RNA interference

The *FOXM1* siRNA sequences #1 and #2 were 5′-CUCUUCUCCCUCAGAUAUAdTdT-3′ and 5′-GGACCACUUUCCCUACUUdTdT-3′, respectively. For stable expression of the *FOXM1* short hairpin RNA, a vector for RNA interference specific to *FOXM1* was constructed based on the piGENE PUR hU6 vector (iGENE Therapeutics, Tsukuba, Japan) according to the manufacturer's instructions (15). The negative control vector, piGENE PUR hU6, supplied by the manufacturer, contains a 66 bp hairpin with limited homology to known sequences in the human genome. The vectors were transfected into cells using the Lipofectamine 2000 kit (Life Technologies, Gaithersburg, MD) according to the manufacturer's instructions.

Reverse transcription–polymerase chain reaction and quantitative real-time polymerase chain reaction

Total RNA was extracted from cells using the RNeasy system (Qiagen, Tokyo, Japan), and 2 μg RNA was reverse transcribed using a first-strand cDNA synthesis kit (Roche, Indianapolis, IN). Polymerase chain reaction was performed using a DNA thermal cycler (model PTC 200; MJ Research, Watertown, MA). Sense and antisense oligonucleotide sequences, respectively, of each primer were as follows: *FOXM1*, (F1) 5′-CACCCCAGTGCCAACCGCTACTTG-3′ and (R1) 5′-AAAGAGGAGCTATCCCCTCCTCAG-3′; *FOXM1A1*, (F2) 5′-GCGACTCTCGAGCATGGAGAATTGTCACCTG-3′ and (R2) 5′-GCGCTACTCGAGTTCGGTTTTGATGGT-3′; *FOXM1A2*, (F3) 5′-GGGCGCACGGCGGAAGATGAA-3′ and (R3) 5′-CCACTCTTCCAAGGGAGGGCTC-3′; *FOXM1B*, (F4) 5′-CCAGGTGTTTAAGCAGCAGAAACGAC-3′ and (R4) 5′-TCAGCTAGCAGCACCTTGGGGGCAAT-3′; *Cyclin B1*, 5′-AAGAGCTTTAAACTTTGGTCTGGG-3′ and 5′-CTTTGTAAGTCCTTGATTTACCATG-3′; *Cdc25B*, 5′-TCTCATCTGAGCGTGGGC-3′ and 5′-CTTCAGGCCTCGAAAGGC-3′; *GAPDH*, 5′-GAACAGCAACGAGTACCGGGTA-3′ and 5′-CCCATGGCCTTGACCAAGGAG-3′. F1/R1 primers can detect all three *FOXM1* isoforms. F2/R2 primers can detect isoforms 1A and 1C and F3/R3 primers specifically detect isoform 1A. *FOXM1A1* sense and antisense primers encompass the A1 exon, whereas *FOXM1A2* sense and antisense primers encompass the A2 exon. *FOXM1B*-specific sense and antisense primers only detect *FOXM1B* that does not express both exon A1 and exon A2. The F4 forward primer spans the spliced out exon A1 and the R4 reverse primer spans the spliced out exon A2. (see Figure 1). Polymerase chain reaction conditions for *FOXM1* and *GAPDH* were 28 cycles of denaturation at 96°C for 30 s, annealing at 56°C for 30 s and extension at 72°C for 30 s. All reverse transcription–polymerase chain reaction (RT–PCR) experiments were performed in duplicate. The primer pairs *FOXM1* F1 and *FOXM1* R1 were used for quantification of *FOXM1* mRNA transcripts. Quantitative real-time–polymerase chain reaction was performed using SYBER Green dye and an ABI PRISM 7700 Sequence detector (Perkin-Elmer/Applied Biosystems, Foster City, CA).

Cell proliferation assay

KG-1, Kasumi-1, U937 and YRK2 cells were transfected with *FOXM1* siRNA #2 or control siRNA or were left untreated. After 3 days incubation, the cells were plated in six-well plates at a density of 1 × 10^4 cells per well. Cell proliferation was measured by counting cells using a hemocytometer. Each data point was performed in triplicate, and the results are reported as mean counts ± SD. Cell viability was also was assessed by counting of viable cells using trypan blue (Sigma–Aldrich) exclusion. The siRNA-transfected, or non-transfected, KG-1, Kasumi-1, U937 and YRK2 cells were stained with trypan blue. The numbers of non-viable cells were determined by counting the cells that showed trypan blue uptake in a hemocytometer and reported as the percentage of untransfected control cells.

Cell cycle analysis

Cellular DNA content was analyzed using propidium iodide (PI) (Sigma–Aldrich) staining. On day 3 post-transfection, the cells were then stained with 50 μg/ml PI. The relative DNA content per cell was measured using flow cytometry and an Epics Elite flow cytometer (Coulter Immunotech, Marseille, France). The percentage of cells in G_1, S and G_2/M phases was calculated using the ModFit program (Becton Dickinson).

Western blot analysis

Cells transfected with control siRNA or *FOXM1* siRNA were harvested after 3 days. Western blot analysis was performed as described (36) using the following antibodies: rabbit polyclonal anti-FOXM1 (MPP2 K-19, 1:500), anti-p27^{Kip1} (1:1000), anti-Skp2 (1:500) and anti-Cdc25B (1:500), all from Santa Cruz. Rabbit polyclonal anti-KIS (1:500) and anti-Aurora-A (1:500) both from ABGENT (San Diego, CA). Mouse monoclonal anti-p21^{Cip1} (1:1000), anti-Cyclin B1 (1:500) and anti-Survivin (1:500), all from Santa Cruz. To ensure equal protein loading, western blotting of actin, used as an internal control, was carried out using a mouse monoclonal anti-actin antibody (1:1000) (C-4; ICN, Aurora, OH).

FOXM1 protein expression analysis

MNCs from leukemia patients and healthy volunteers were fixed and permeabilized using the IntraStain kit (DakoCytomation, Glostrup, Denmark) according to the manufacturer's instructions. FOXM1 protein expression was detected using a FOXM1 rabbit polyclonal antibody as a primary antibody and an fluorescein isothiocyanate (FITC)-conjugated monoclonal mouse anti-rabbit immunoglobulin G1 (IgG1) (DakoCytomation) as the secondary antibody. FOXM1 protein expression levels were evaluated as mean fluorescence intensities.

Immunofluorescence microscopy

Cells were cytocentrifuged onto glass slides, fixed and permeabilized. The cells were incubated with a diluted FOXM1 rabbit polyclonal antibody as the primary antibody and then incubated with an FITC-conjugated monoclonal mouse anti-rabbit IgG1 as the secondary antibody. PI (Sigma–Aldrich) was used to stain the nuclei. The cells were viewed using phase contrast and fluorescence microscopy (IMT-2; Olympus, Tokyo, Japan).

Colony-forming assays

Colony-forming assays were performed by plating purified populations of cells at concentrations ranging from 1 × 10^3 to 2 × 10^3 into methylcellulose media (Methocut H4435: Stem Cell Technologies). Colonies were enumerated under light microscopy (Zeiss, Munchen, Germany) following incubation for 14 days at 37°C and 5% CO_2.

Isolation of progenitor cells and quantitative real-time–polymerase chain reaction of progenitor cells

Following colony formation, each colony was harvested using a glass syringe, and all cells of the same colony were pooled and washed. An RNeasy system was used to extract total RNA from ~5 × 10^4 cells from each colony.

Statistical analysis

Data are representative of at least three experiments with essentially similar results. These results are expressed as the means ± SD from three independent experiments. The means were compared using Student's t-test. P values <0.05 were considered statistically significant.

Results

The expression of FOXM1 mRNA isoforms in AML cells

The *FOXM1* mRNA contains 10 exons, 2 of which are alternatively expressed, giving rise to 3 differentially expressed mRNA isoforms

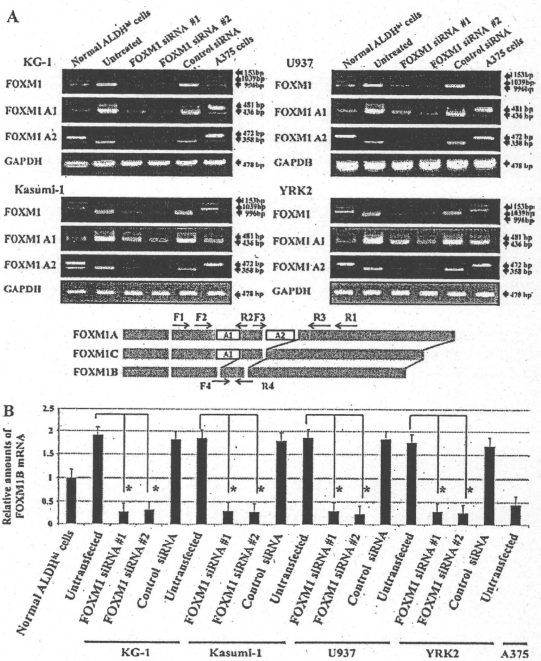

Fig. 1. *FOXM1* mRNA expression in leukemia cells. (A) RT–PCR analysis of the expression of the mRNAs encoding the three isoforms of *FOXM1* in normal ALDH^{hi} cells, in A375 melanoma cells (positive control) and in KG-1, Kasumi-1, U937 and YRK2 leukemic cell lines that were either not transfected or transfected with *FOXM1* siRNA #1 or #2 or with control siRNA. RT–PCR was performed using the three pairs of *FOXM1* primers indicated at bottom. The representative gel images show the PCR products amplified using the indicated primer pairs: *FOXM1*, F1 and R1 (detects all isoforms), *FOXM1A1*, F2 and R2, (exon A1, detects isoforms 1A and 1C) or *FOXM1A2*, F3 and R3 (exon A2, detects isoform 1A only) primer pairs; respective positions are indicated on the left of the gel images. The siRNA-transfected cells were assayed 3 days after transfection. RT–PCR was performed to detect *FOXM1* mRNAs. *GAPDH* was assayed as an internal control. RT–PCR results are representative of three independent experiments. A375 melanoma cell line as positive control for *FOXM1A* mRNA expression. Bottom panels: schematic representation of the genomic structure of the *FOXM1* gene. The *FOXM1* gene consists of two alternatively expressed exons (A1 and A2) that generate three alternatively spliced coding isoforms (15). The respective positions of the RT–PCR primer pairs are indicated on the *FOXM1* gene (15). (B) Relative levels of *FOXM1B* mRNA expression in siRNA-transfected cells using *FOXM1B*-specific primers (F4 and R4). The amounts of total *FOXM1B* mRNA in KG-1, Kasumi-1, U937 and YRK2 cells, that were not transfected or were transfected with the indicated siRNAs, were assessed using quantitative RT–PCR. The siRNA-transfected cells were assayed 3 days after transfection. The mRNA expression levels were normalized to the expression of *GAPDH* mRNA in the same sample and the results are expressed relative to normal ALDH^{hi} cells, which were assigned a value of 1. Each RT–PCR assay was performed at least three times, and the results are expressed as means ± SD. $^{*}P < 0.01$ compared with untreated control cells.

(*FOXM1A*, *FOXM1B* and *FOXM1C*) (7). *FOXM1A* contains both alternative exons, *FOXM1B* contains none of the alternative exons and *FOXM1C* only contains exon *A1*. We determined the relative expression of the three *FOXM1* isoforms in normal ALDH^{hi} cells and in leukemia cell lines, using three pairs of primers (*FOXM1* F1 and R1, *FOXM1A1* F2 and R2 and *FOXM1A2* F3 and R3) that were designed to amplify across the two alternatively expressed A1 and A2 exons and across individual exons A1 and A2, respectively (outlined in Figure 1A). As shown in Figure 1A, all three mRNA isoforms were detectable by RT–PCR. The *FOXM1* mRNA that was predominantly expressed in KG-1, Kasumni-1, U937 and YRK2 cells was the *FOXM1B* isoform. The expression of *FOXM1C* mRNA was weakly detected in all leukemia cell lines. In contrast, *FOXM1A* mRNA expression was not detected in leukemia cell lines. Weak expression of *FOXM1A*, *FOXM1B* and *FOXM1C* mRNA was detected in normal ALDH^{hi} cells. Total *FOXM1* mRNA expression in leukemia cells was higher than that of normal ALDH^{hi} cells. In leukemia cells, *FOXM1B* mRNA accounted for almost all the *FOXM1* mRNA expression. To further analyze the role of *FOXM1* in these cells, we knocked down *FOXM1* using two different siRNAs. These siRNAs decreased the mRNA expression of total *FOXM1* and of the *FOXM1A1* and *FOXM1A2* isoforms in leukemia cells (Figure 1A). Moreover, we performed a quantitative RT–PCR for detection of *FOXM1B* isoform using *FOXM1B*-specific primers (F4 and R4) that will only detect *FOXM1B* that does not express both exon A1 and exon A2 (outlined in Figure 1A) to investigate the relative expression of *FOXM1B* mRNA in KG-1, Kasumi-1, U937 and YRK2 cells using A375 cells as a positive control. This analysis indicated that the expression of

FOXM1B mRNA in these leukemia cells was increased 1.79- to 1.91-fold relative to its expression in normal $ALDH^{bi}$ cells. Leukemia cells transfected with *FOXM1* siRNA #1 or #2 showed decreases in *FOXM1B* mRNA expression of 0.24- to 0.33-fold relative to its expression in untreated leukemia cells (Figure 1B).

Effects of FOXM1 knockdown on AML cell proliferation

To examine the functional importance of FOXM1 expression, we transfected KG-1, Kasumi-1, U937 and YRK2 cells with *FOXM1* siRNA #2 and assessed the effects of FOXM1 knockdown on AML cell proliferation over 72 h of culture, starting from 3 days post-transfection (Figure 2, upper panels). Cell proliferation was measured by counting cells using a hemocytometer. When AML cells were transfected with *FOXM1* siRNA #2, cell proliferation was significantly reduced compared with both untreated cells and to control siRNA-transfected cells. However, the cell viability of AML cells transfected with *FOXM1* siRNA #2 was almost same as that of both untreated cells and control siRNA-transfected cells (Figure 2, middle panels). These results show that FOXM1 plays an important role in AML cell proliferation.

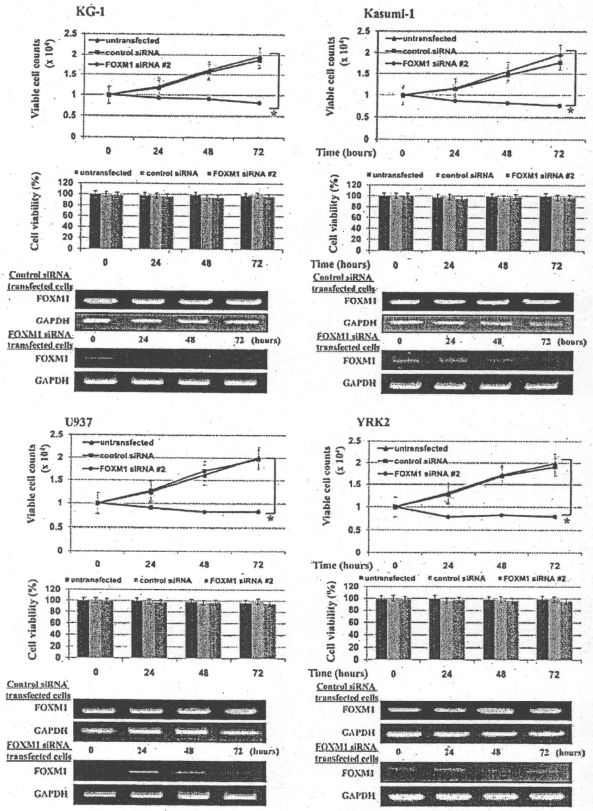

Fig. 2. Effect of *FOXM1* siRNA transfection on cell proliferation and viability of leukemia cell lines. Top panel: cell proliferation of KG-1, Kasumi-1, U937 and YRK2 cells, transfected with control siRNA or with *FOXM1* siRNA #2, was measured by counting cells using a hemocytometer. The cell counting was started 3 days after transfection and was performed every 24 h for 3 days. Data are shown as means ± SD of triplicate cultures and are representative of three independent experiments. $^*P < 0.01$ compared with untreated control cells. Middle panels: cell viability of the KG-1, Kasumi-1, U937 and YRK2 cells in the upper panel was assessed by counting of viable cells using trypan blue staining at 0, 24, 48 and 72 h, starting 3 days after siRNA transfection. The untransfected cells (dark gray bars), control siRNA-transfected cells (light gray bars) and *FOXM1* siRNA #2-transfected cells (mid gray bars). Bottom panels: expression of *FOXM1* mRNA or control *GAPDH* mRNA in control siRNA or *FOXM1* siRNA #2-transfected cells, at each time point was assessed using RT–PCR. The RT–PCR results are representative of three independent experiments.

Knockdown of FOXM1 induced cell cycle arrest in AML cells

We further examined the effect of FOXM1 knockdown on AML cell proliferation by FACS analysis of the effect of FOXM1 on cell cycle stage. As shown in Figure 3, analysis of KG-1, Kasumi-1, U937 and YRK2 cells on day 3 post RNA interference transfection indicated an increase in the percentage of cells in G_2/M and a decrease in the G_1 and S populations compared with untreated or control scrambled RNA-treated cells. No increase in the sub-G_1 population of these cells was observed. Interestingly, we also detected an increase (2.1–3.6%) in the percentage of polyploid cells (>4N) in FOXM1-siRNA compared with control cells (Figure 3). These results showed that knockdown of FOXM1 induced a block in G_2/M in the AML cells, but did not induce apoptosis, and therefore demonstrated that reduction of FOXM1 expression strongly inhibited AML cell proliferation.

FOXM1 is essential for cell cycle progression in AML cells

We next determined if the inhibitory effect of FOXM1 knockdown on cell proliferation was mediated by modulation of the expression of cell cycle regulators, such as $p27^{Kip1}$, $p21^{Cip1}$, Skp2, Cdc25B, Cyclin B1, Survivin, KIS, Aurora B kinase or Aurora A kinase. As shown in Figure 4, depletion of the FOXM1 protein in FOXM1 siRNA #2-transfected KG-1, Kasumi-1, U937 and YRK2 cells was accompanied by a significant reduction in the levels of Skp2, Cdc25B, KIS, Aurora B kinase, Cyclin B1 and Survivin proteins compared with

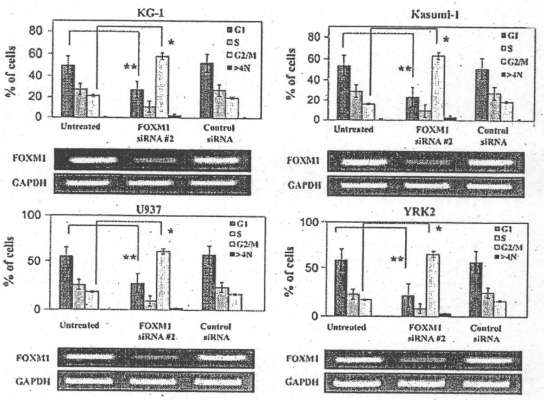

Fig. 3. Effect of *FOXM1* siRNA on the cell cycle of transfected AML cells. The cell cycle stage and ploidy of KG-1, Kasumi-1, U937 and YRK2 cells that were untreated, or were transfected with *FOXM1* siRNA #2 or control siRNA, were analyzed using FACS analysis. The siRNA-transfected cells were harvested after 3 days. The fraction of cells in the G_1 (dark gray bars), S (mid gray bars) and G_2/M (light gray bars) stage of the cell cycle and the fraction of cells that exhibited polyploidy (>4N, black bars) were determined. Data are shown as means ± SD of triplicate cultures. The *FOXM1* mRNA expression of each cell line is shown at bottom and was assessed using RT–PCR. The RT–PCR results are representative of three independent experiments. $^{*}P < 0.01$ compared with untreated control cells. $^{**}P < 0.05$ compared with untreated control cells.

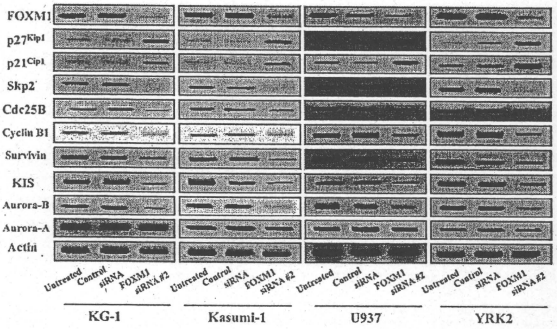

Fig. 4. Effect of FOXM1 knockdown on the expression of cell cycle-regulating proteins in leukemia cell lines. KG-1, Kasumi-1, U937 and YRK2 cells were either left untreated or were transfected with control siRNA or with *FOXM1* siRNA #2. The cells were harvested after 3 days, and the expression of the indicated cell cycle-regulating proteins was analyzed by SDS–PAGE followed by western blotting using the specific antibodies. Blotting of actin was used as a loading control.

untreated or control siRNA-transfected leukemia cells. In contrast, suppression of FOXM1 protein expression did not inhibit the expression of Aurora A kinase and resulted in increased levels of $p27^{Kip1}$ and $p21^{Cip1}$ proteins. These results indicate that FOXM1 transcription factor is essential for the expression of cell cycle regulatory proteins in AML cells.

FOXM1 mRNA expression in ALDH^{hi} cell populations from AML patients

We next examined *FOXM1* mRNA expression in clinical specimens from AML patients. Hematopoietic progenitor cells from the bone marrow of healthy volunteers (n = 20) were obtained by flow cytometric sorting of these cells according to their aldehyde dehydrogenase activity. ALDH^{hi} hematopoietic progenitor cells, which include $CD34^+$, $CD133^+$, c-kit^+ and Lin^- cells, were selected according to their side scatter and FITC properties. The ALDH^{hi}-selected populations of healthy volunteers represented 0.43% of the MNCs of the bone marrow. Representative FACS data from one healthy volunteer are shown in Figure 5A (left panel, gated by black circle). We also isolated ALDH^{hi} cells from the bone marrow of AML patients [*n* = 127; M1 (n = 21), M2 (n = 56), M4 (n = 32) and M5 (n = 18)] using the gated region. Representative data from AML patients (AML; M2 #5 and M5 #7) are shown in Figure 5A (middle and right panels). The ALDH^{hi}-selected populations of AML patients (M2 #5 and M5 #7) represented 54.2 and 37.1%, respectively, of the MNCs of the bone marrow. These percentages were almost equal to the percentages of leukemic blast counts in peripheral blood. Thus, the ALDH^{hi} cell count indirectly indicated the count of leukemic blast cells in AML samples. We analyzed *FOXM1* mRNA expression in the ALDH^{hi} populations of 20 normal ALDH^{hi} cell populations and in a total of 127 primary AML-derived ALDH^{hi} populations using quantitative RT–PCR. Representative relative *FOXM1* mRNA expression and the corresponding RT–PCR product gel patterns are shown for four normal individuals and for 15 AML patients in Figure 5B (upper and lower panels respectively). A comparison of the *FOXM1* mRNA expression levels of all AML-derived ALDH^{hi} samples assayed with that in all normal ALDH^{hi} cells assayed is shown in Figure 5C. *FOXM1* mRNA was more strongly expressed in all AML-derived ALDH^{hi} populations compared with its expression in normal ALDH^{hi} cells. There were no significant differences in the induction of *FOXM1* mRNA expression among the AML specimens. The mean ratios of *FOXM1* mRNA expression to that of the internal control *GAPDH* in AML specimens were 2.14 ± 0.31 (M1), 2.26 ± 0.47 (M2), 1.65 ± 0.42 (M4) and 1.92 ± 0.38 (M5). In contrast, the mean ratio of *FOXM1/GAPDH* mRNA expression in normal ALDH^{hi} cells was 1.0 ± 0.16. These results demonstrated that there was no significant difference in the expression level of *FOXM1* among various leukemia specimens and that *FOXM1* mRNA levels were increased in almost all of the various leukemia specimens analyzed compared with the levels in normal ALDH^{hi} cells.

Comparison of FOXM1 protein expression in leukemia and normal cells

To confirm that the high mRNA expression of *FOXM1* in leukemia cells was associated with high FOXM1 protein expression, we next examined FOXM1 protein expression in ALDH^{hi} cells derived from healthy volunteers and from AML patients using immunofluorescent staining. FOXM1 protein expression was quantified using an anti-FOXM1 antibody and a FITC-conjugated secondary antibody, followed by FACS analysis and quantification of the fluorescence intensity. Representative flow cytometry analysis of FOXM1 protein expression of AML-derived ALDH^{hi} cells (M1 #3, M2 #5, M4 #5 and M5 #7) and normal ALDH^{hi} cells (#5) are shown in Figure 5D. FOXM1 expression in AML-derived ALDH^{hi} cells was higher than normal ALDH^{hi} cells. Moreover, FOXM1 median mean fluorescence intensity values were higher in the ALDH^{hi} cells derived from all 35 AML patients (M1 #3, 197 ± 16.2; M2 #5, 212 ± 17.3; M4 #5, 165 ± 26.7 and M5 #7, 183 ± 30.5) than in the ALDH^{hi} cells derived from 20 normal controls (42.7 ± 4.4). FOXM1 protein expression was not significantly different between AML subgroups (M1 to M5) (Figure 5E). Furthermore, FOXM1 median mean fluorescence intensity values of ALDH^{hi} cells derived from bone marrow and peripheral blood MNCs of AML patients were also not significantly different (data not shown). Coimmunofluorescent staining of FOXM1 with the nuclear marker PI revealed that FOXM1 was constitutively present in the nucleus in both AML and normal cells. However, the FOXM1 protein was more strongly expressed in AML-derived ALDH^{hi} cells than in normal ALDH^{hi} cells. Representative data of AML patients (AML; M2 #5) and normal controls (normal #2) are shown in Figure 6F. These findings showed that, similar to the AML cell lines analyzed above, FOXM1 is more strongly expressed in leukemia cells and is therefore probably to promote the proliferation of these cells.

Depletion of FOXM1 inhibited colony formation of ALDH^{hi} cells derived from AML patients

To confirm that FOXM1 also modulated the proliferation of AML cells from patients, we analyzed the effect of FOXM1 knockdown on colony formation of ALDH^{hi} cells from normal healthy volunteers and AML patients prior to treatment (Figure 6). Transfection of *FOXM1* siRNA induced a dramatic decrease in the numbers of colonies formed by AML-derived ALDH^{hi} cells compared with those in untreated or control scrambled RNA-treated cells. The inhibition of colony formation was similar for all AML cells. In contrast, colony formation of normal ALDH^{hi} cells was only slightly reduced by transfection with *FOXM1* siRNA compared with control cells (Figure 6A and B). These results demonstrate that inhibition of *FOXM1* expression inhibited the proliferation of AML-derived ALDH^{hi} cells.

To confirm that FOXM1 inhibition of colony formation of AML cells derived from patients was mediated by an effect on the transcription of FOXM1 target genes, we assayed the mRNA expression of the FOXM1 target genes *Cyclin B* and *Cdc25B* using RT–PCR and compared their expression between AML-derived and normal ALDH^{hi} cells. As shown in Figure 6C and D, depletion of *FOXM1* expression significantly decreased the expression of *Cyclin B* and *Cdc25B* mRNA in AML-derived ALDH^{hi} cells. In contrast, depletion of FOXM1 only moderately decreased the expression of *Cyclin B* and *Cdc25B* mRNA in normal ALDH^{hi} cells. These findings suggest that *FOXM1* is strongly expressed in AML-derived ALDH^{hi} cells and that FOXM1 depletion had a stronger effect on these cells than on normal ALDH^{hi} cells. Moreover, these data indicate that a greater reduction in the expression of both *CyclinB* and *Cdc25B* is observed in AML-derived ALDH^{hi} cells than in normal ALDH^{hi} cells following the siRNA-induced decrease in *FOXM1* expression.

Discussion

FOXM1 plays important roles in cell proliferation, differentiation and apoptosis (1,10,23). Moreover, the FOXM1 gene is aberrantly expressed and activated in many human malignancies (11,12,14,15,19–21). However, the function of aberrant FOXM1 expression in AML cells is unknown. In the present study, we aimed to gain more insight into how FOXM1 regulates AML cell proliferation. We showed that the *FOXM1* gene was overexpressed in AML cells and that depletion of FOXM1 inhibited AML cell proliferation. Our results provide *in vitro* evidence to support a role for *FOXM1* as an oncogene in AML cells and to support the fact that its downregulation inhibits the proliferation of established AML cell lines and primary AML cells.

We found that the *FOXM1B* isoform was predominantly expressed in AML cells. Using transient transfection of *FOXM1* siRNA, we showed that reducing FOXM1 expression inhibited leukemia cell proliferation and induced an increase in the population of leukemia cells at the G_2/M phase compared with control siRNA transfected or untreated cells, 3 days after transfection. These data are consistent with the established notion that the *FOXM1B* isoform is a key regulator of G_2/M progression (9,10,14,18,37,38). These previous data indicate that FOXM1B is activated by Cyclin B1/Cdk1 in late

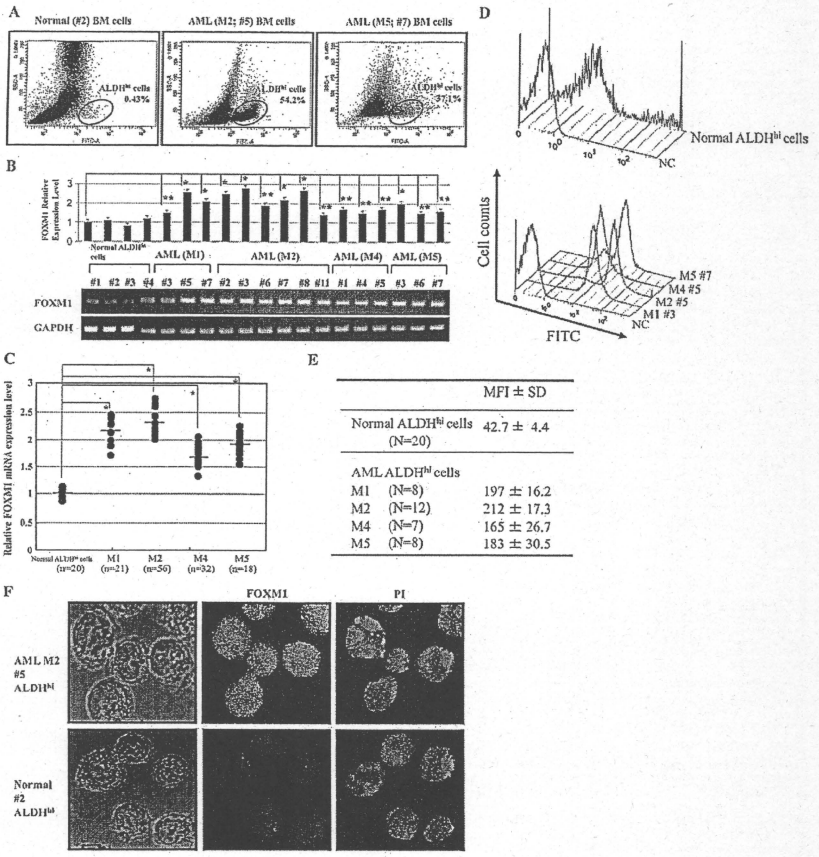

		MFI ± SD
Normal ALDH^{hi} cells (N=20)		42.7 ± 4.4
AML ALDH^{hi} cells		
M1	(N=8)	197 ± 16.2
M2	(N=12)	212 ± 17.3
M4	(N=7)	165 ± 26.7
M5	(N=8)	183 ± 30.5

Fig. 5. *FOXM1* mRNA expression in ALDH^{hi} cells isolated from AML patients. (A) ALDH^{hi} cells were obtained from the bone marrow of healthy volunteers (n = 20) and 127 AML patients (M1, n = 21; M2, n = 56; M4, n = 32 and M5, n = 18) by FACS sorting. Representative FACS data of one healthy volunteer and two AML patients (M2 #5 and M5 #7) are shown. The collected fractions are the parts gating with the black circle. (B) Quantitative RT–PCR analysis of *FOXM1* mRNA expression in ALDH^{hi} cells derived from four representative healthy volunteers and representative AML patients (M1: #3, #5 and #7; M2: #2, #3, #6, #7, #8 and #11; M4: #1, #4 and #5 and M5: #3, #6 and #7) (upper panel). Gel analysis of the RT–PCR products is shown at bottom. The levels of the quantified RT–PCR products were normalized to *GAPDH* expression in the same sample and were then expressed relative to the mRNA level of a normal control, which was assigned a value of 1. $^{*}P < 0.01$ compared with normal ALDH^{hi} cells. $^{**}P < 0.05$ compared with normal ALDH^{hi} cells. (C) The *FOXI* mRNA level of all the indicated 127 AML patients, as well as 20 normal controls, was quantified as in B. Each RT–PCR assay was performed at least three times. Each dot represents an individual patient. The horizontal bar represents the median mRNA level for each group. $^{*}P < 0.01$ compared with normal ALDH^{hi} cells. (D) FOXM1 protein expression in ALDH^{hi} cells from representative normal individuals and from individuals with AML was analyzed using a FITC-conjugated FOXM1 antibody and flow cytometry. The results are representative of three independent experiments. NC, negative control. The normal ALDH^{hi} cells were derived from healthy volunteer #5. The AML-derived ALDH^{hi} cells were derived from patients M1 #3, M2 #5, M4 #5 and M5 #7. (E) Summary of FOXM1 protein expression levels of normal ALDH^{hi} cells (n = 20) and of ALDH^{hi} cells derived from patients with AML (M1, n = 8; M2, n = 12; M4, n = 7 and M5, n = 8). FOXM1 protein expression is expressed as the mean fluorescence intensity (MFI). The MFI ± SD was calculated for each group. (F) Immunofluorescence analysis of FOXM1 protein expression in ALDH^{hi} cells from AML M2 patient #5 (top panel) and from healthy volunteer #2 (bottom panel). The cells were fixed in 4% paraformaldehyde. After washing, the cells were resolved and were then permeabilized. The cells were incubated with a diluted FOXM1 antibody and were then washed and incubated with an FITC-conjugated monoclonal mouse anti-rabbit immunoglobulin G1 secondary antibody (green). Nuclei were stained using PI (red). The cells were viewed using phase contrast (left panels) and fluorescence microscopy. Original magnification ×400.

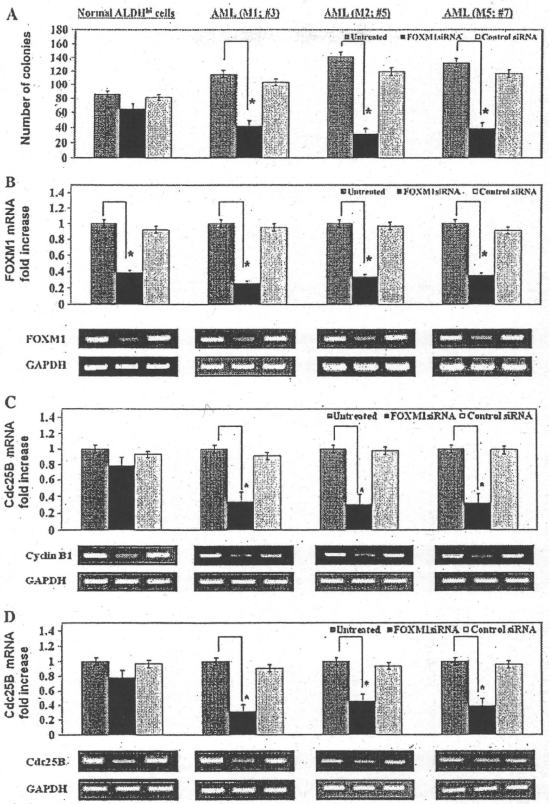

Fig. 6. *FOXM1* expression in ALDH^{hi} cells derived from AML patients. ALDH^{hi} cells were purified from one healthy volunteer and three AML patients (AML: M1, #3; M2, #5 and M5, #7) and were cultured in semisolid methylcellulose media. The ALDH^{hi} cells from each source were either untransfected (untreated) or were transfected with control siRNA or *FOXM1* siRNA. After 14 days culture, the cells were then analyzed for colony-forming ability (A) or for the mRNA expression of *FOXM1* (B), *cyclin B1* (C) or *Cdc25B* (D) using quantitative RT–PCR and RT–PCR. (A) The number of colonies formed by each group was counted. For normal ALDH^{hi} cells, the mean number of colonies in untreated cells was 86 (73–91), in *FOXM1* siRNA-transfected cells was 65 (59–74) and in control siRNA-transfected cells was 81 (67–85). In the AML cells, the mean number of colonies in M1 #3, M2 #5 and M5 #7, respectively, was 115 (101–118), 141 (129–156) and 132 (121–149) in untreated cells; 42 (32–48), 32 (25–36) and 39 (28–41) in *FOXM1* siRNA-treated cells and 103 (93–109), 119 (113–126) and 116 (110–121) in control scrambled RNA-treated cells. These numbers represent the number of individual colonies produced per 1000 cells plated for doses ranging from 1×10^3 to 2×10^3 ALDH^{hi} cells. The results are the means ± SD of three independent experiments. $^*P < 0.01$ compared with untreated control cells. (B), (C) and (D) The results of quantitative RT–PCR analysis of the mRNA expression of the *FOXM1* mRNA (B), *cyclin B1* mRNA (C) and *Cdc25B* mRNA (D) were normalized relative to the *GAPDH* mRNA level in the same sample. The fold increase in each mRNA relative to the untreated control of each sample, which was assigned a value of 1, was calculated. Data are shown as the means ± SD of triplicate cultures and are representative of three independent experiments. Gel analysis of the RT–PCR products are shown in the bottom panels. The RT–PCR results are representative of three independent experiments.

G_2 and M phases and that this activation correlates with FOXM1-mediated stimulation of the G_2/M transition and with activation of genes with positive roles in the G_2/M transition and in mitosis (18,29,39). In contrast to FOXM1B activation in the G_2/M phase, the FOXM1C isoform is activated by the G_1 phase proliferation signal Cyclin D1/Cdk4, and this activation of FOXM1C correlates with FOXM1C stimulation of the G_1/S transition and with activation of genes that promote the G_1/S transition and S phase progression (29,40). It has been also reported that FOXM1C is abundantly expressed in a variety of primary and secondary cultured cell lines (28,41,42). However, in this study, we found that FOXM1C is only weakly expressed in AML cells and the *FOXM1* isoform that was

predominantly expressed in AML cells was the *FOXM1B* mRNA isoform. These results were similar to previous reports (43,44). We also found that knockdown of FOXM1 weakly induced mitotic catastrophe.

Because siRNA-mediated depletion of FOXM1 expression induced G_2/M cell cycle arrest and inhibited AML cell proliferation, we hypothesized that identification of genes regulated by FOXM1 would facilitate an understanding of the roles FOXM1 plays in AML cell proliferation. We showed that the knockdown of FOXM1 diminished the expression of $p27^{Kip1}$ and $p21^{Cip1}$ proteins, which are known to have negative effects on the cell cycle machinery by binding to various Cyclin/Cdk complexes and inhibiting their activities (45). Knockdown of FOXM1 markedly decreased the protein expression of the mitotic regulators Skp2, Cdc25B, Cyclin B1, Survivin, KIS and Aurora-B kinase in AML cells. Diminished expression of these mitotic regulators results in a block in mitotic progression or proliferation and leads to an accumulation of $p27^{Kip1}$ and $p21^{Cip1}$ proteins. However, the reasons why knockdown of FOXM1 predominantly induced G_2/M cell cycle arrest rather than G_1 cell cycle arrest in AML cells remain unclear. One reason may be that FOXM1 associates with different cell cycle-regulating complexes at different stages of the cell cycle. It has been reported that FOXM1 associates with Cyclin E/Cdk2 complexes in the G_1 and S phases of cell cycle, whereas it preferentially binds the Cyclin B1/Cdk1 complex in the G_2 phase (39). A second possible reason is that FOXM1 is regulated differently at different cell cycle stages. FOXM1 transcriptional activity is maintained at a low level during G_1/S through the action of its N-terminal autoinhibitory domain, and Cyclin A/Cdk complexes are required to phosphorylate and activate FOXM1 during G_2 phase (46). The transcriptional activity of exogenous FOXM1 is higher in G_2/M synchronized than in G_1/S-arrested cells (18). Moreover, it has been reported that inhibition of proliferation is associated with a decrease in the expression of Cdc25B and with increased $p21^{Cip1}$ gene expression in myeloid leukemia cells (25). The Cdc25B phosphatase participates in the G_2/M checkpoint recovery and its expression is upregulated in AML cells (47). The expression of $p21^{Cip1}$ caused strong G_2 arrest and resumed leukemia cell cycle progression (48). The progressive increase in the transcriptional activity of FOXM1 during cell cycle progression is explained by its subsequent activation by the Cyclin/Cdk complexes, such as CyclinB/Cdk1, which become active in late G_2 phase (39). The Aurora kinases play an important role in chromosome alignment, segregation and cytokinesis during mitosis. Aurora kinase A and B have been reported to be aberrantly expressed in 15 different human leukemia cell lines, such as PALL-1, PALL-2, HL-60, NB4 and MV4-11, as well as in freshly isolated leukemia cells from 44 individuals with acute myelogenous leukemia (49). FOXM1 regulates the transcriptional activation of the Aurora B kinase gene, which is crucial for mitotic entry, and a polyploidy genotype has been observed in FOXM1-deficient cells (12,13). Thus, FOXM1 predominantly controls expression of a subset of genes in the G_2/M-specific gene cluster, among which are essential regulators of mitosis. Therefore, depletion of FOXM1 might be expected to strongly induce G_2/M cell cycle arrest in AML cells.

A major finding of this study is that FOXM1 mRNA expression in the $ALDH^{hi}$ cells of patients of AML (127/127; 100%) is aberrant, being significantly higher than that of healthy volunteers. Probably, the most important finding of our study is that FOXM1 protein expression was higher in $ALDH^{hi}$ cells derived from AML patients (n = 35) than in normal $ALDH^{hi}$ cells. Our data suggest that FOXM1 protein expression may be associated with leukemia cell proliferation in AML patients. Moreover, knockdown of FOXM1 expression in $ALDH^{hi}$ cells derived from AML patients dramatically decreased the median number of colonies formed. In addition, depletion of FOXM1 reduced *Cyclin B1* and *Cdc25B* mRNA expression, resulting in inhibition of the proliferation of AML-derived $ALDH^{hi}$ cells. These results demonstrate that inhibition of FOXM1 inhibits AML $ALDH^{hi}$ progenitor cell proliferation through induction of G_2/M cell cycle arrest.

In summary, this study shows, for the first time, that FOXM1 is aberrantly expressed in AML cells and has an important role in their proliferation. We showed that inhibition of FOXM1 represents an attractive target for leukemia therapy.

Funding

Grant-in-Aid for scientific research (No. 17590987) from the Ministry of Education, Culture, Sports, Science, and Technology of Japan.

Acknowledgements

Conflict of Interest Statement: None declared.

References

1. Carlsson,P. *et al.* (2002) Forkhead transcription factors: key players in development and metabolism. *Dev. Biol.*, **250**, 1–23.
2. Clark,K.L. *et al.* (1993) Co-crystal structure of the HNF-3/fork head DNA-recognition motif resembles histone H5. *Nature*, **364**, 412–420.
3. Kaestner,K.H. *et al.* (2000) Unified nomenclature for the winged helix/forkhead transcription factors. *Genes Dev.*, **14**, 142–146.
4. Marsden,I. *et al.* (1998) Structural changes in the region directly adjacent to the DNA-binding helix highlight a possible mechanism to explain the observed changes in the sequence-specific binding of winged helix proteins. *J. Mol. Biol.*, **278**, 293–299.
5. Korver,W. *et al.* (1997) The human TRIDENT/HFH-11/FKHL16 gene: structure, localization, and promoter characterization. *Genomics*, **46**, 435–442.
6. Yao,K.M. *et al.* (1997) Molecular analysis of a novel winged helix protein. WIN. *J. Biol. Chem.*, **272**, 19827–19836.
7. Luscher-Firzlaff,J.M. *et al.* (1999) Interaction of the fork head domain transcription factor MPP2 with the human papilloma virus 16 E7 protein: enhancement of transformation and transactivation. *Oncogene*, **18**, 5620–5630.
8. Ye,H. *et al.* (1997) Hepatocyte nuc.ear factor 3/fork head homolog 11 is expressed in proliferating epithelial and mesenchymal cells of embryonic and adult tissues. *Mol. Cell. Biol.*, **17**, 1626–1641.
9. Ye,H. *et al.* (1999) Premature expression of the winged helix transcription factor HFH-11B in regenerating mouse liver accelerates hepatocyte entry into S-phase. *Mol. Cell. Biol.*, **19**, 8570–8580.
10. Wang,X. *et al.* (2002) The Forkhead Box m1b transcription factor is essential for hepatocyte DNA replication and mitosis during mouse liver regeneration. *Proc. Natl Acad. Sci. USA*, **99**, 16881–16886.
11. Kalin,T.V. *et al.* (2006) Increased levels of the FoxM1 transcription factor accelerate development and progression of prostate carcinomas in both TRAMP and LADY transgenic mice. *Cancer Res.*, **66**, 1712–1720.
12. Kim,I.M. *et al.* (2006) The Forkhead Box m1 transcription factor stimulates the proliferation of tumor cells during development of lung cancer. *Cancer Res.*, **66**, 2153–2161.
13. Krupczak-Hollis,K. *et al.* (2004) The mouse Forkhead Box m1 transcription factor is essential for hepatoblast mitosis and development of intrahepatic bile ducts and vessels during liver morphogenesis. *Dev. Biol.*, **276**, 74–88.
14. Wonsey,D.R. *et al.* (2005) Loss of the forkhead transcription factor FoxM1 causes centrosome amplification and mitotic catastrophe. *Cancer Res.*, **65**, 5181–5189.
15. Wang,I.C. *et al.* Forkhead box M1 regulated the transcriptional network of genes essential for mitotic progression and genes encoding the SCF (Skp2-Cks1) ubiquitin ligase.. *Mol. Cell. Biol.*, **25**, 10875–10894.
16. Kalinichenko,V.V. *et al.* (2003) Ubiquitous expression of the forkhead box M1B transgene accelerates proliferation of distinct pulmonary cell types following lung injury. *J. Boil. Chem.*, **278**, 37888–37894.
17. Wang,X. *et al.* (2002) Increased hepatic Forkhead Box M1B (FoxM1B) levels in old-aged mice stimulated liver regeneration through diminished p27Kip1 protein levels and increased Cdc25B expression. *J. Biol. Chem.*, **277**, 44310–44316.
18. Laoukili,J. *et al.* (2005) FoxM1 is required for execution of the mitotic programme and chromosome stability. *Nat. Cell Biol.*, **7**, 126–136.
19. Kalinichenko,V.V. *et al.* (2004) Foxm1b transcription factor is essential for development of hepatocellular carcinomas and is negatively regulated by the p19ARF tumor suppressor. *Genes Dev.*, **18**, 830–850.
20. Liu,M. *et al.* (2006) FoxM1B is overexpression in human glioblastomas and critically regulates the tumorigenicity of glioma cells. *Cancer Res.*, **66**, 3593–3602.
21. Yoshida,Y. *et al.* (2007) The forkhead box M1 transcription factor contributes to the development and growth of mouse colorectal cancer. *Gastroenterology*, **132**, 1420–1431.

22. Heselmeyer,K. *et al.* (1997) Advanced-stage cervical carcinomas are defined by a recurrent pattern of chromosomal aberrations revealing high genetic instability and a consistent gain of chromosome arm 3q. *Genes Chromosomes Cancer*, **19**, 233–240.
23. Laoukili,J. *et al.* (2007) FoxM1: at the crossroads of ageing and cancer. *Biochim. Biophys. Acta*, **1775**, 92–102.
24. Spirin,K.S. *et al.* (1996) p27/Kip1 mutation found in breast cancer. *Cancer Res.*, **56**, 2400–2404.
25. Rodriguez,S. *et al.* (2005) Conventional and array-based comparative genomic hybridization analysis of nasopharyngeal carcinomas from the Mediterranean area. *Cancer Genet. Cytogenet.*, **157**, 140–147.
26. Singh,B. *et al.* (2001) Molecular cytogenetic characterization of head and neck squamous cell carcinoma and refinement of 3q amplification. *Cancer Res.*, **61**, 4506–4513.
27. Zettl,A. *et al.* (2004) Genomic profiling of peripheral T-cell lymphoma, unspecified, and anaplastic large T-cell lymphoma delineates novel recurrent chromosomal alterations. *Am. J. Pathol.*, **164**, 1837–1848.
28. Teh,M.T. *et al.* (2002) FOXM1 is a downstream target of Gli1 in basal cell carcinomas. *Cancer Res.*, **62**, 4773–4780.
29. Wierstra,I. *et al.* (2007) FOXM1, a typical proliferation-associated transcription factor. *Biol. Chem.*, **388**, 1257–1274.
30. Myatt,S.S. *et al.* (2007) The emerging roles of forkhead box (Fox) proteins in cancer. *Nat. Rev. Cancer*, **7**, 847–859.
31. Korver,W. *et al.* (1997) The winged-helix transcription factor trident is expressed in actively dividing lymphocytes. *Immunobiology*, **198**, 157–161.
32. Lowenberg,B. *et al.* (1999) Acute myeloid leukemia. *N. Engl. J. Med.*, **341**, 1051–1062.
33. Radosevic,N. *et al.* (2001) Cell cycle regulatory protein expression in fresh acute myeloid leukemia cells and after drug exposure. *Leukemia*, **15**, 559–566.
34. McArthur,G.A. *et al.* (2002) MAD1 and p27 (KIP1) cooperate to promote terminal differentiation of granulocytes and to inhibit Myc expression and cyclin E-CDK2 activity. *Mol. Cell. Biol.*, **22**, 3014–3024.
35. Radosevic,N. *et al.* (2001) Cell cycle regulatory protein expression in fresh acute myeloid leukemia cells and after drug exposure. *Leukemia*, **4**, 559–566.
36. Nakamura,S. *et al.* (2008) KIS induces proliferation and the cell cycle progression through the phosphorylation of p27Kip1 in leukemia cells. *Leuk. Res.*, **32**, 1358–1365.
37. Korver,W. *et al.* (1998) Uncoupling of S phase and mitosis in cardiomyocytes and hepatocytes lacking the winged-helix transcription factor. *Trident. Curr. Boil.*, **8**, 1327–1330.
38. Leung,T.W. *et al.* (2001) Over-expression of FoxM1 stimulates cyclin B1 expression. *FEBS Lett.*, **507**, 59–66.
39. Majot,M.L. *et al.* (2004) Forkhead Box M1B transcriptional activity requires binding of Cdk-cyclin complexes for phosphorylation-dependent recruitment of p300/CBP coactivators. *Mol. Cell. Biol.*, **7**, 1455–1469.
40. Wierstra,I. *et al.* (007) The central domain of transcription factor FOXM1c directly interacts with itself *in vivo* and switches from an essential to an inhibitory domain depending on the FOXM1c binding site. *Boil. Chem.*, **388**, 805–818.
41. Li,S.K. *et al.* (2008) FoxM1c counteracts oxidative stress-induced senescence and stimulates Bmi-1 expression. *J. Biol. Chem.*, **283**, 16545–16553.
42. Ma,R.Y. *et al.* (2005) Ra0f/MEK/MAPK signaling stimulates the nuclear translocation and transactivating activity of FOXM1c. *J. Cell Sci.*, **118**, 795–806.
43. Gemenetzidis,E. *et al.* (2009) FOXM1 upregulation is an early event in human squamous cell carcinoma and it is enhanced by nicotine during malignant transformation. *PLoS ONE*, **44**, e4849.
44. Yokomine,K. *et al.* (2010) The forkhead box M1 transcription factor as a candidate of target for anti-cancer immunotherapy. *Int. J. Cancer*, **126**, 2153–2163.
45. Sherr,C.J. (1993) Mammalian G1 cyclins. *Cell*, **73**, 1059–1065.
46. Laoukili,J. *et al.* (2008) Activation of FoxM1 during G2 requires cyclin A/Cdk-dependent relief of autorepression by the FoxM1 N-terminal domain. *Mol. Cell. Biol.*, **28**, 3076–3087.
47. Didier,C. *et al.* (2008) G2/M checkpoint stringency is a key parameter in the sensitivity of AML cells to genotoxic stress. *Oncogene*, **27**, 3811–3820.
48. Bunz,F. *et al.* (1998) Requirement for p53 and p21 to sustain G2 arrest after DNA damage. *Science*, **282**, 1497–1501.
49. Ikezoe,T. *et al.* (2007) A novel treatment strategy targeting Aurora kinases in acute myelogenous leukemia. *Mol. Cancer Ther.*, **6**, 1851–1859.

Received March 7, 2010; revised August 24, 2010; accepted August 27, 2010

Int J Hematol (2010) 92:664–666
DOI 10.1007/s12185-010-0706-6

CASE REPORT

Expanded distribution of the T315I mutation among hematopoietic stem cells and progenitors in a chronic myeloid leukemia patient during imatinib treatment

Yosuke Minami · Tomohiro Kajiguchi · Akihiro Abe · Toshihito Ohno · Hitoshi Kiyoi · Tomoki Naoe

Received: 26 April 2010 / Revised: 7 September 2010 / Accepted: 4 October 2010 / Published online: 22 October 2010

Abstract T315I mutation of the ABL-kinase domain in chronic myeloid leukemia (CML) confers resistance to imatinib (IM) as well as second-generation tyrosine kinase inhibitors (TKIs). We report a chronic-phase CML patient undergoing IM treatment, who showed the overt existence of the T315I mutation after 15 months. We retrospectively analyzed the distribution of the T315I mutation using the invader assay and direct DNA sequencing among FACSAria-sorted populations from bone marrow cells: total mononuclear cells (TMC), hematopoietic stem cells (HSC)/Thy-1$^+$, HSC/Thy-1$^-$, common myeloid progenitors (CMP), granulocyte macrophage progenitors (GMP), and megakaryocyte erythroid progenitors (MEP), at 0, 3, 6, 9, and 12 months after IM treatment. T315I was barely detectable by 12 months in TMC, but detectable in 19.2% of HSC/Thy-1$^-$ and 46.4% of MEP at diagnosis, and finally expanded into all populations. These results suggest that the monitoring of gene mutations in HSC and progenitors at diagnosis might be helpful for the early detection of TKI-resistant CML patients and facilitate appropriate therapeutic decision.

Keywords Chronic myeloid leukemia · Imatinib · T315I · BCR-ABL

1 Introduction

Patients who carry the T315I mutation in BCR-ABL are unresponsive to imatinib (IM) as well as second-generation tyrosine kinase inhibitors (TKIs); this mutation might, therefore, represent an important pathway for chronic myeloid leukemia (CML) cells [1–3]. There are several unanswered questions about the T315I mutation: Are T315I-mutated clones invariably selected in the presence of IM, and should all patients be screened for T315I mutation with highly sensitive assays? In this article, we report a CML patient in whom the distribution of the T315I mutation expanded among each cell population, including hematopoietic stem cells (HSC) and progenitors, during IM treatment.

2 Case report

In July 2008, a 41-year-old Japanese man was diagnosed with chronic-phase CML. The Sokal score was 0.67, showing low risk (age, 41 years; hypochondrial spleen size, 0 cm; platelet number, 147 × 10^3/mL; blast cells in peripheral white blood cells, 2%). On G-banding examination, there were no additional chromosomal abnormalities other than t(9;22)(q34;q11). The standard first line therapy (imatinib: 400 mg/day, p.o.) was started with favorable tolerability. He agreed to participate in a clinical observation study regarding residual *BCR-ABL* transcripts using real-time qPCR assays among FACSAria-sorted populations of bone marrow cells:

Y. Minami and T. Kajiguchi contributed equally.

Y. Minami (✉) · A. Abe · T. Naoe
Department of Hematology and Oncology,
Nagoya University Graduate School of Medicine,
65 Tsurumai-cho, Showa-ku, Nagoya 466-8550, Japan
e-mail: yminami@med.nagoya-u.ac.jp

T. Kajiguchi · T. Ohno
Department of Hematology, Tosei General Hospital,
Seto, Japan

H. Kiyoi
Department of Infectious Disease, Nagoya University
School of Medicine, Nagoya, Japan

total mononuclear cells (TMC), HSC/Thy-1$^+$, HSC/Thy-1$^-$, common myeloid progenitors (CMP), granulocyte macrophage progenitors (GMP), and megakaryocyte erythroid progenitors (MEP), at 0, 3, 6, 9, and 12 months after IM treatment [4, 5]. After 6 months of IM treatment, the proportion of myeloid progenitors changed from an MEP-dominant pattern to a pattern similar to normal bone marrow cells (Fig. 1a), as previously shown [4, 5]. However, the ratio of MEP gradually increased after 12 months. Regarding transcripts of *BCR-ABL/BCR* in the total mononuclear cells derived from bone marrow cells, a decrease was observed for 6 months, but had almost stopped at the 12-month examination (Fig. 1b). He achieved a complete hematologic response (CHR) at 3 months and a partial cytogenetic response (PCyR) at 6 months; however, a complete cytogenetic response (CCyR) was not seen at 12 months. According to the European LeukemiaNet criteria [6], he showed an optimal response until 6 months and a suboptimal response at 12 months (without a consideration of gene mutations described later). After 12 months, an escalation dose of imatinib (600 mg/day, p.o.) was used until 15 months; however, PCyR and CHR were finally lost (failure based on the European LeukemiaNet criteria), and we planned to switch to the second TKI treatment. Before starting, we examined ABL-kinase mutations in bone marrow cells, and observed the overt existence of the T315I mutation at the ABL-kinase domain by direct sequence and invader assay analyses. We are now preparing to perform allogeneic hematopoietic stem cell transplantation from his HLA-identical sibling.

We preserved cDNA from each population for the qPCR assays involving *BCR-ABL/BCR*. Based on his consent (all examinations of residual *BCR-ABL* transcripts and ABL-kinase mutations were performed according to the approval of the institutional review boards of Nagoya University and Tosei General Hospital), we retrospectively analyzed the gene mutations at the ABL-kinase domain. At diagnosis, T315I mutation already existed in 19.2% of HSC/Thy-1$^-$ and 46.4% of MEP populations (Fig. 2). We investigated each population, and the results showed limited existence of the T315I mutation only in progenitors and HSC (and in MNC temporally at 3 months), but it finally expanded into all populations during IM treatment (Table 1).

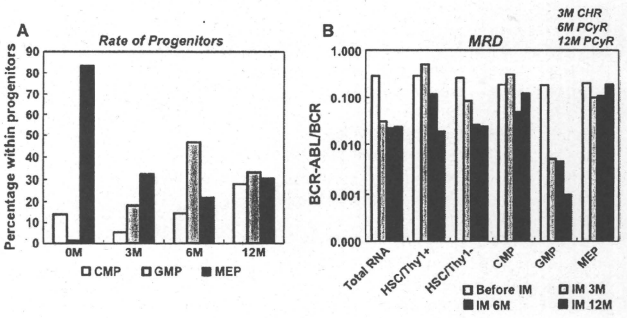

Fig. 1 **a** Analysis of the proportion of progenitors including common myeloid progenitors (CMP), granulocyte–macrophage progenitors (GMP), and megakaryocyte–erythroid progenitors (MEP). The percentage of individual progenitors within the CD34$^+$CD38$^-$Lin$^-$ population is shown. **b** The minimum residual diseases (MRD) using quantitative PCR for *BCR-ABL/BCR* among each population. *CHR* complete hematologic response; *PCyR* partial cytogenetic response

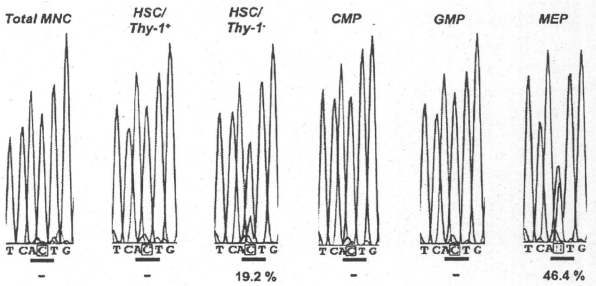

Fig. 2 Distribution of T315I mutations at diagnosis. Percentages were calculated based on the height of each peak for the mutation and wild-type

Table 1 Distribution of T315I mutations during imatinib (IM) treatment

	0 M	3 M	6 M	9 M	12 M	15 M
Total MNC	wild type	T315I 20%	wild type	wild type		
HSC/Thy−1+	wild type	wild type	wild type	T315I 20%		
HSC/Thy−1−	T315I 20%		wild type	T315I 10%	T315I 20%	
CMP	wild type	T315I 30%	wild type	T315I 10%		
GMP	wild type	T315I 40%	wild type	wild type		
MEP			T315I 10%	T315I 30%		

< 3%
< 50%
< 100%
≒100%

Percentages were calculated as shown in Fig. 2 and rounded off

3 Discussion

Jiang et al. [7] showed that, in 20–33% of cDNA preparations from freshly isolated CML stem cell-enriched populations, both allele specific amplification and direct sequencing methods revealed the existence of mutations at the ABL-kinase domain. In the study, primary CML stem cells displayed instability of the *BCR-ABL* fusion gene in vivo and in vitro, and so some patients may possess leukemic stem cells with ABL-kinase mutations before the initiation of TKI treatment. There is another report that low-level T315I mutation was detectable in CP-CML patients prior to IM therapy, and the mutation could be clonally selected, causing IM resistance [8]. On the other hand, there is a publication that low-level mutations (including T315I mutation) at diagnosis were not always clonally selected during IM therapy [9, 10]. In our case, ABL-kinase mutations in HSC populations were not detected at 6 months (Table 1). It is possible that some immunosurveillance systems also worked for rare T315I-mutated clones, or technical limitations regarding sensitivity affected the result with the invader assay and direct DNA sequencing methods. In addition, MEP seemed to contain T315I-positive cells more frequently than the HSC populations in this case. In the mathematical model, acquired mutations at the ABL-kinase domain were frequently produced at the progenitor level, and they could ultimately be resistant clones [11]. The mathematical simulation is compatible with our observation. It is important to clarify the source of CML stem cells and resistant clones during TKIs-treatment.

Although we need to observe more cases and investigate clinical study settings to assess the significance, the present case suggests that monitoring gene mutations in HSC and progenitors at diagnosis might be helpful for the early detection of TKI-resistant CML patients and making appropriate therapeutic decisions.

Acknowledgments We thank Yuka Nomura at Nagoya University for her technical assistance. This study was supported by Grants-in-Aid from the National Institute of Biomedical Innovation and from the Ministry of Education, Culture, Sports, Science and Technology on Scientific Research.

References

1. Nicolini FE, Mauro MJ, Martinelli G, Kim DW, Soverini S, Muller MC, et al. Epidemiologic study on survival of chronic myeloid leukemia and Ph+ acute lymphoblastic leukemia patients with BCR-ABL T315I mutation. Blood. 2009;114:5271–8.
2. Quintas-Cardama A, Kantarjian H, Cortes J. Imatinib and beyond-exploring the full potential of targeted therapy for CML. Nat Rev Clin Oncol. 2009;6:535–43.
3. Branford S, Melo JV, Hughes TP. Selecting optimal second-line tyrosine kinase inhibitor therapy for chronic myeloid leukemia patients after imatinib failure: does the BCR-ABL mutation status really matter? Blood. 2009;114:5426–35.
4. Jamieson CH, Ailles LE, Dylla SJ, Muijtjens M, Jones C, Zehnder JL, et al. Granulocyte-macrophage progenitors as candidate leukemic stem cells in blast-crisis CML. N Engl J Med. 2004;351:657–67.
5. Abe A, Minami Y, Hayakawa F, Kitamura K, Nomura Y, Murata M, et al. Retention but significant reduction of BCR-ABL transcript in hematopoietic stem cells in chronic myelogenous leukemia after imatinib therapy. Int J Hematol. 2008;88:471–5.
6. Baccarani M, Cortes J, Pane F, Niederwieser D, Saglio G, Apperley J, et al. Chronic myeloid leukemia: an update of concepts and management recommendations of European LeukemiaNet. J Clin Oncol. 2009;27:6041–51.
7. Jiang X, Saw KM, Eaves A, Eaves C. Instability of BCR-ABL gene in primary and cultured chronic myeloid leukemia stem cells. J Natl Cancer Inst. 2007;99:680–93.
8. Roche-Lestienne C, Laï JL, Darré S, Facon T, Preudhomme C. A mutation conferring resistance to imatinib at the time of diagnosis of chronic myelogenous leukemia. N Engl J Med. 2003;348:2265–6.
9. Lange T, Park B, Willis SG, Deininger MW. BCR-ABL kinase mutations in chronic myeloid leukemia: not quite enough to cause resistance to imatinib therapy? Cell Cycle. 2005;4:1761–6.
10. Sherbenou DW, Wong MJ, Humayun A, McGreevey LS, Harrell P, Yang R, et al. Mutations of the BCR-ABL-kinase domain occur in a minority of patients with stable complete cytogenetic response to imatinib. Leukemia. 2007;21:489–93.
11. Michor F. Mathematical models of cancer stem cells. J Clin Oncol. 2008;26:2854–61.

Int J Hematol (2010) 92:624–633
DOI 10.1007/s12185-010-0692-8

ORIGINAL ARTICLE

Selective KIT inhibitor KI-328 and HSP90 inhibitor show different potency against the type of KIT mutations recurrently identified in acute myeloid leukemia

Akane Tsujimura · Hitoshi Kiyoi · Yukimasa Shiotsu · Yuichi Ishikawa · Yumiko Mori · Hiroshi Ishida · Tsutomu Toki · Etsuro Ito · Tomoki Naoe

Received: 7 July 2010 / Revised: 31 August 2010 / Accepted: 13 September 2010 / Published online: 5 October 2010

Abstract Activating mutations of KIT play an important role in the pathophysiology of several human malignancies, including acute myeloid leukemia. Activated KIT kinase is therefore a promising molecular target for the treatment of many malignancies harboring KIT activation. Here we examined the potency of a novel KIT inhibitor KI-328 against different types of mutant KIT kinases recurrently identified in AML. KI-328 shows selective potency against KIT kinase for the in vitro kinase assay, and inhibits the growth of wild-type (Wt)- and mutant-KIT-expressing cells, while it has little potency against D816V-KIT. Comparable analysis of several potent KIT inhibitors regarding growth inhibitory effects on a variety of mutant-KIT-expressing cells revealed that multi-kinase inhibitors have the same potency against D816V-KIT as other mutant KITs; however, the predominant potency against D816V-KIT was observed in heat shock protein 90 (HSP90) inhibitors. Furthermore, HSP90 inhibitors suppress the growth of D816V-KIT-expressing cells at the concentration at which the growth of other mutant-KIT-expressing cells is not affected. These results collectively indicated that potent KIT inhibitors have different potency against the type of mutant KIT kinases. Therefore, KIT inhibitors are required to validate potency against several types of mutant KIT kinases for the clinical development.

Keywords KIT · Tyrosine kinase · Inhibitor · HSP90 · Leukemia

1 Introduction

KIT is a class III receptor tyrosine kinase (RTK) together with FLT3, FMS and platelet-derived growth factor receptor (PDGFR), and is the receptor for stem cell factor (SCF) [1, 2]. Binding of SCF to KIT induces kinase activity through dimerization and tyrosine phosphorylation, resulting in the activation of downstream molecules, such as PI3K/AKT, STAT3 and MAP kinase (MAPK), which is involved in cell proliferation and survival [3, 4]. KIT expression has been demonstrated in a variety of human malignancies, such as mastocytosis, gastrointestinal stromal tumor (GIST), and acute myeloid leukemia (AML), and the kinase activity of KIT is involved in their development and progression [5–7]. Several mechanisms for activating KIT kinase have been demonstrated in malignant cells, while activating mutations of KIT play an important role in the pathophysiology of mastocytosis, GIST and AML [8, 9]. KIT mutations are found at the most in 5% of unselected AML patients, while they are frequently identified in core binding factor (CBF)-AML, which is characterized by t(8;21)(q22;q22), inv(16)(p13q22) and t(16;16)(p13;q22) [10–13]. Although CBF-AML has been stratified into a favorable karyotype risk group, several studies have

A. Tsujimura · Y. Ishikawa · Y. Mori · T. Naoe
Department of Hematology and Oncology,
Nagoya University Graduate School of Medicine,
Nagoya, Japan

A. Tsujimura · H. Kiyoi (✉) · Y. Ishikawa · Y. Mori
Department of Infectious Diseases, Nagoya University School of Medicine, Tsurumai-cho 65, Showa-ku,
Nagoya 466-8560, Japan
e-mail: kiyoi@med.nagoya-u.ac.jp

Y. Shiotsu · H. Ishida
Kyowa Hakko Kirin, Fuji Research Park, Shizuoka, Japan

T. Toki · E. Ito
Department of Pediatrics, Hirosaki University
Graduate School of Medicine, Hirosaki, Japan

demonstrated the possible adverse effects of KIT mutations on the outcome of CBF-AML [14–16]. These observations therefore strongly indicate that activated KIT kinase is a promising molecular target for the treatment of many malignancies harboring KIT activation [17].

Although several small molecule compounds have been disclosed to have potency against KIT kinase, their potency against mutant KIT differs among mutations [18–25]. To date, many mutations have been identified in the different regions of KIT, and there seems to be a tendency toward a skewed mutated region according to the tumor type [9]. In AML, KIT mutations are mainly identified in three different regions; exon 8 in the extra-cellular domain, exon 10–11 in the transmembrane and juxtamembrane domains, and exon 17 in the kinase domain, and prognostic implications reportedly differed among mutation types [14–16]. Therefore, it is necessary to evaluate their potency against each type of mutant KIT for the clinical development of KIT inhibitors. Furthermore, multiple KIT mutations reportedly induced resistance against several KIT kinase inhibitors, such as imatinib in GIST [26], requiring the validation of alternative strategies that can inhibit constitutively activated KIT kinases. One strategy is to enhance the cellular degradation of activated KIT proteins. It has been shown that KIT is a client protein of heat shock protein 90 (HSP90), and HSP90 inhibitors substantially reduced phosphorylation levels of activated KIT through the degradation of KIT proteins [27, 28]. Therefore, HSP90 inhibitors might serve as therapeutic agents against AML with KIT mutations.

Recently, we have developed a novel KIT-selective inhibitor KI-328 by the further modification of the compound 7d, which was a pyrimidine derivative identified during the development of FLT3 inhibitors [29]. In this study, we evaluated its potency against different types of mutant KIT kinases, the mutations of which are recurrently identified in AML, in comparison with SCF-dependent wild-type (Wt)-KIT kinase. Furthermore, we evaluated the potency of HSP90 inhibitors against mutant KIT proteins.

2 Materials and methods

2.1 Reagents

KI-328 and FI-197 were synthesized in the Kyowa Hakko Kirin (Shizuoka, Japan). FI-197 is a derivative compound of KI-328, and has a multiple potency against several tyrosine kinases in addition to KIT. Geldanamycin and 17-AAG were purchased from Sigma–Aldrich (St Louis, MO). Reagents were prepared as a 10 mM dimethylsulfoxide (DMSO) solution, stored at −20°C until use, and freshly diluted with cell culture medium.

2.2 Kinase inhibition profile

The in vitro kinase assays were performed according to the KinaseProfilerTM Assay Protocols of Upstate Biotechnology (Lake Placid, NY).

2.3 Cell lines and cell culture

Human leukemia cell lines, MV4;11 and K562 were obtained from the American Type Culture Collection (Manassas, VA), Kasumi-1 was from Hiroshima University (Hiroshima, Japan), and MegO1 was established at Nagoya University. MV4;11 was maintained in Iscove's Modified Dulbecco's Medium (IMDM) (Invitrogen, Carlsbad, CA) supplemented with 10% fetal calf serum (FCS) (Invitrogen), and the other human leukemia cell lines were in RPMI1640 medium (Invitrogen) supplemented with 10% FCS. It has been found that MV4;11 has internal tandem duplication of the *FLT3* gene (FLT3/ITD), K562 and MegO1 have *BCR-ABL* translocation, Kasumi-1 has *RUNX1-RUNX1T1* translocation and N822K *KIT* mutation. A murine IL3-dependent myeloid progenitor cell line, 32D, was obtained from the RIKEN cell bank (Tsukuba, Japan), and maintained in RPMI1640 medium supplemented with 10% FCS and 1 ng/ml murine IL3 (R&D Systems, Minneapolis, MN).

2.4 Establishment of mutant-KIT-expressing 32D cells

Cloning of the full-length human KIT cDNA was reported previously [30]. Five KIT mutations [T417F with deletions of 418 and 419 residues (T417FA2AA) at exon 8, V540L and M541L at exon 10, D816V and N822K at exon 17] were identified by screening the bone marrow cells obtained from AML patients, as previously reported [12]. Among these mutations, the M541L mutation has been reported as a polymorphism [31]. Informed consent was obtained from all patients to use their samples for the present study as well as banking and molecular analysis, and approval was obtained from the ethics committees of Nagoya University. Each mutated full-length KIT cDNA was generated by replacing each corresponding region of Wt-KIT cDNA. Wt- and mutated-KIT cDNAs were cloned into the pMX-IP vector (kindly provided by Professor Toshio Kitamura, Tokyo University, Japan), transduced into 32D cells, as previously described [32], and established stable Wt- and mutated-KIT-expressing 32D cells. Stable expression of KIT protein in each cell line was confirmed by Western blotting using anti-KIT antibody (Santa Cruz Biotechnology, Santa Cruz, CA) as well as its surface expression by flow cytometry using anti-KIT antibody (Pharmingen, San Diego, CA). We also established

the pMX-IP vector-transfected 32D cells (mock-32D) as a control.

2.5 Growth inhibition and cell cycle analyses

Cell lines and established 32D cells were suspended in RPMI1640 medium containing 10% FCS with or without human SCF (R&D Systems), and 2×10^4 cells per well were seeded in 96-well culture plates with or without each inhibitor. Cell viability was measured using the CellTiter96 Proliferation Assay (Promega, Madison, WI) according to the manufacturer's instructions. These procedures were performed three times independently.

For cell cycle analysis, Wt- and mutated-KIT-expressing 32D cells (1×10^5) were treated with increasing concentrations of KI-328 for 24 h. DNA contents were analyzed as previously described [33].

2.6 Colony formation analysis

Wt- and mutated-KIT-expressing 32D cells (1×10^5 cells) were plated in MethoCult methylcellulose semi-solid medium (M3231; StemCell Technologies, Vancouver, BC) with or without human SCF or KI-328, and then incubated at 37°C for 14 days. Human AML cells (1×10^5 cells) were plated in MethoCult methylcellulose semi-solid medium containing human SCF, GM-CSF and IL-3 (H4534; StemCell Technologies) with or without KI-328 and 17-AAG, then incubated at 37°C for 14 days. Colonies with >20 cells were scored using an inverted microscope.

2.7 Differentiation analysis of mutant-KIT-expressing 32D cells

For the induction of myeloid differentiation, each 32D cell line was washed three times with the RPMI1640 medium containing 10% FCS and re-suspended in RPMI1640 medium containing 10% FCS and 30 ng/ml recombinant G-CSF with or without 1 ng/ml murine IL3 or 50 ng/ml human SCF. After 5, 7 and 10 days of culture, cells were cytospun and subjected to staining for Wright–Giemsa staining.

2.8 Western blot

Wt- and mutant-KIT-expressing 32D cells were treated with inhibitors for 24 h, and cell pellets were suspended with lysis buffer. Equal amounts of whole cell lysates were separated by SDS-polyacrylamide gel electrophoresis, and electroblotted onto Immobilon PVDF membranes (Millipore, Bedford, MA). Immunoblotting was performed with anti-phospho-KIT, anti-phospho-STAT3, anti-phospho-AKT and anti-phospho-MAPK antibodies (Cell Signaling, Danvers, MA). Signals were developed using an ECL system (GE Healthcare, Uppsala, Sweden). The membranes were incubated with stripping buffer, and then reprobed with anti-KIT (Santa Cruz Biotechnology), anti-STAT3, anti-AKT and anti-MAPK (Cell Signaling) antibodies. For the immunoprecipitation of KIT and HSP90 proteins, each lysate was incubated with anti-KIT or anti-HSP90 antibody (Santa Cruz Biotechnology), and then precipitated by Protein A Sepharose (GE Healthcare) as previously described [34].

3 Results

3.1 Selective kinase inhibition by KI-328

A novel small molecule KIT kinase inhibitor, KI-328, was identified by screening and modification of the chemical libraries of Kyowa Hakko Kirin. The chemical structure of KI-328 is shown in Fig. 1a. KI-328 inhibited KIT kinase with an IC_{50} of 0.34 μM for the in vitro kinase assay. The selectivity of KI-328 was examined against a wide range of kinases (Table 1). Among them, more than 50% of inhibition was observed against only KIT kinase at the 1 μM of KI-328.

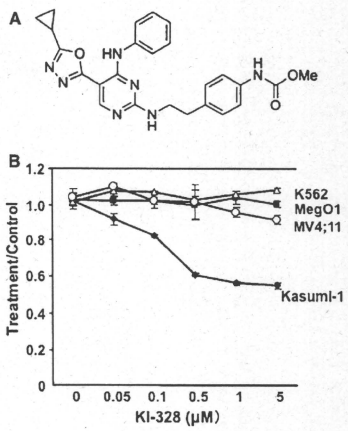

Fig. 1 Structure and growth inhibitory effect of KI-328 on human leukemia cell lines. **a** Chemical structure of KI-328. **b** Growth inhibitory effect on human leukemia cell lines was evaluated by measuring viable cells after treatment with KI-328 for 72 h. KI-328 selectively inhibits the growth of Kasumi-1, which has a N822K KIT mutation

Table 1 Kinase inhibitory profile of KI-328 in vitro

Enzyme	Inhibitory activity at 1 μM (%)
KIT	76
FGFR	45
PDGFRβ	36
RAF	33
ABL	9
SRC	7
FLT3	6
CDK2	3
EGFR	1
PKCβI	0
PKA	0
CK2	0

Consistent with the kinase inhibitory profile, KI-328 potently inhibited the proliferation of Kasumi-1 cells (GI_{50}, 0.52 μM), which has a N822K-KIT mutation, but not other leukemia cell lines harboring *FLT3* or *BCR-ABL* mutations (Fig. 1b).

3.2 Establishment of Wt- and mutant-KIT-expressing 32D cells

We established Wt- and five mutant (T417FΔ2AA, V540L, M541L, D816V and N822K) KIT-expressing 32D cells. Stable expression of Wt- and each mutant KIT protein was confirmed by flow cytometry and Western blotting (Fig. 2a, b). Although Wt- and M541L-KIT proteins were SCF-dependently phosphorylated, T417FΔ2AA-, V540L-, D816V- and N822K-KIT proteins were constitutively phosphorylated; however, the phosphorylation levels of T417FΔ2AA-, V540L- and N822K-KIT proteins were lower than that of D816V-KIT. SCF stimulation increased the phosphorylation levels of T417FΔ2AA-, V540L- and N822K-KIT proteins to the same level of D816V-KIT, while it did not affect the phosphorylation level of D816V-KIT (Fig. 2b).

Next we examined the proliferation abilities of Wt- and mutant-KIT-expressing 32D cells. D816V-KIT-expressing 32D cells showed autonomous proliferation without the presence of either IL3 or SCF, while the other mutant-KIT-expressing 32D cells required stimulation with IL3 or SCF for proliferation in contrast to the constitutive phosphorylations of their KIT proteins. However, T417FΔ2AA-, V540L- and N822K-KIT-expressing 32D cells could proliferate at a lower concentration of IL3 (under 0.01 ng/ml), at which Wt- and M541L-KIT-expressing 32D cells could not proliferate (Fig. 2c). To confirm the proliferation abilities of Wt- and mutant-KIT-expressing cells obtained by the liquid culture, they were further examined in a semi-solid culture. Consistent with the results by the liquid culture, only D816V-KIT-expressing 32D cells showed colony formation without stimulation with IL3 or SCF, and T417FΔ2AA-, V540L- and N822K-KIT-expressing 32D cells required stimulation with IL3 or SCF at the lower concentration for colony formation (Fig. 2d). We also examined the G-CSF-mediated granulocytic differentiation in Wt- and mutant-KIT-expressing 32D cells. Mature neutrophils were observed at most in 32% of D816V-KIT-expressing 32D cells after co-culture with G-CSF for 7 days, while at 72–78% in other mutant- and Wt-KIT-expressing cells (Fig. 2e). These results collectively indicated that transforming activities for autonomous proliferation and differentiation block in 32D cells were different among the types of mutant KIT. In addition, M541L-KIT did not show any transforming activity, coinciding with the previous report that this mutation is a polymorphism.

3.3 Growth inhibitory effects of KI-328

To evaluate the sensitivity of KI-328 in the cellular system, we examined the growth inhibitory effects on Wt- and mutant-KIT-expressing 32D cells. Since Wt-, T417FΔ2AA-, V540L-, M541L- and N822K-KIT-expressing 32D cells required IL3 or SCF for proliferation, we evaluate growth inhibitory effects in the presence of 50 ng/ml SCF. Cells were treated with increasing concentrations of KI-328 for 72 h, and then viable cells were determined by the CellTiter96 Proliferation Assay. KI-328 inhibited the growth of Wt-, T417FΔ2AA-, V540L-, M541L- and N822K-KIT-expressing 32D cells with GI_{50} values of 0.127, 0.445, 0.575, 0.229 and 0.967 μM, respectively, but not that of D816V-KIT-expressing cells even at 1.0 μM (Fig. 3a). Furthermore, KI-328 could not inhibit the growth of D816V-KIT-expressing cells even in the condition without SCF stimulation.

3.4 Inhibitory effects of KI-328 on KIT and downstream signals

Wt- and mutant-KIT-expressing 32D cells were treated with increasing concentrations of KI-328 for 6 h. Cell lysates were subjected to Western blot analysis to detect the phosphorylation status of KIT, STAT3, AKT and MAPK. KI-328 suppressed the SCF-dependent phosphorylations of Wt-, T417FΔ2AA-, V540L-, M541L- and N822K-KIT as well as downstream molecules, STAT3, AKT and MAPK, in a dose-dependent manner, and their dephosphorylation were observed at concentrations of over the GI_{50} value against each 32D cell (Fig. 3b). These results indicated

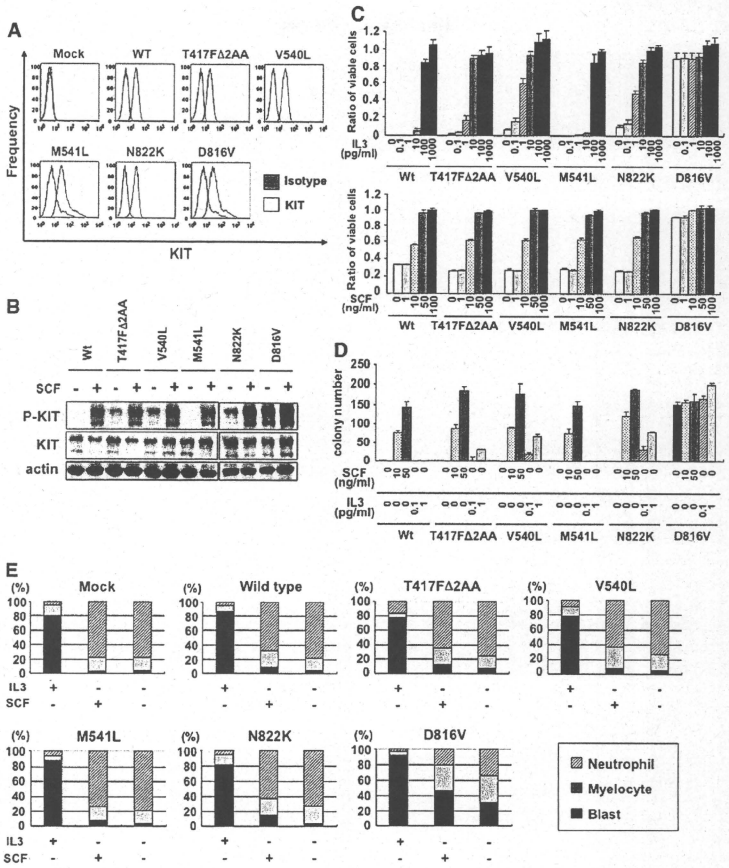

Fig. 2 Characteristics of Wt- and mutant-KIT-expressing 32D cells in proliferation and differentiation. **a** Stable surface expression of each KIT protein was confirmed by flow cytometry. **b** Wt- and M541L-KIT proteins are SCF-dependently phosphorylated, while other mutant KITs are constitutively phosphorylated. **c** Only D816V-KIT-expressing 32D cells can proliferate without IL3 and SCF, while other mutant-KIT-expressing cells do not show the factor-independent proliferation. However, T417FΔ2AA-, V540L- and N822K-KIT-expressing 32D cells could proliferate at a lower concentration of IL3 (under 0.01 ng/mL), at which Wt- and M541L-KIT-expressing 32D cells could not proliferate. Ratio of viable cell number of each KIT-expressing 32D cells to mock-32D cells is presented. **d** The proliferation ability obtained by the liquid culture (c) was confirmed by analysis in semi-solid medium. **e** G-CSF-mediated granulocytic differentiation was evaluated. Only D816V-KIT inhibits maturation

that KI-328 inhibited the growth of Wt-, T417FΔ2AA-, V540L-, M541L- and N822K-KIT-expressing cells by the dephosphorylation of each activated KIT kinase. However, consistent with the growth inhibitory effect, more than 2 μM of KI-328 was required for the dephosphorylation of constitutively active D816V-KIT kinase (Fig. 3b).